

was restored around 7 T, and became larger and shifted to lower energy with increasing the field. Figure 1 illustrates this phenomenon as a field expansion of the PL spectrum every 2 T. We interpret these phenomena in the following scenario: (1) The exciton PL vanishes when the band electron level becomes

higher than the d -electron level with increasing pressure and the energy transfer from the former to the latter is induced, (2) The PL is restored when the band electron level becomes lower than the d -electron level as a result of a Zeeman shift with increasing field.

MAGNETISM & MAGNETIC MATERIALS

Electrical Noise in $\text{La}_{2/3}\text{Sr}_{1/3}\text{MnO}_3$

Anane, A., FSU, Center for Materials Research and Technology (MARTECH)

Raquet, B., FSU, MARTECH and Institut National des Sciences Appliqués (INSA)-Toulouse-France

von Molnár, S., NHMFL/FSU, MARTECH

The current interest in the mixed valance perovskite manganites was originally fueled by the rediscovery of colossal magnetoresistance (CMR) in certain members of this group of materials.¹ The study of the physics of the manganites has, however, progressed far beyond CMR alone. Manganites have offered a fertile ground for the study of spin-charge interactions and transport-magnetism correlations. Furthermore, a multiphase description, where the insulator metal transition occurs via percolation has been proposed.² This picture of the coexistence of metallic and insulating phases, even in samples optimally doped to have the highest T_C , has recently been confirmed experimentally by Scanning Tunneling Microscopy (STM).³

Electrical noise results from transitions of switching entities called "fluctuators." These transitions occur between states that have different conductivity. Studying the temperature and field dependence of the noise can provide insight into the electrical and magnetic nature of the fluctuators. Therefore, it is an effective tool for probing the dynamic behavior of an electrically inhomogeneous system, such as the manganites.

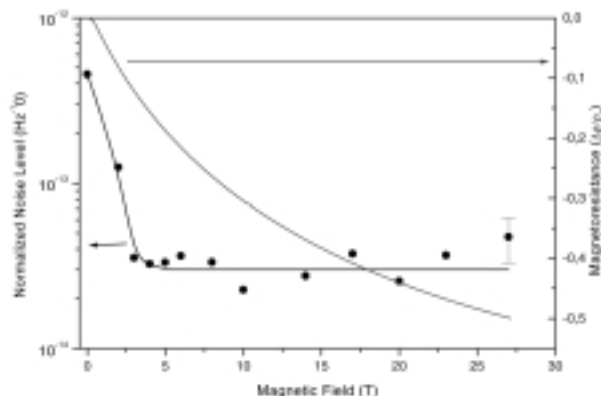


Figure 1. Magnetic field dependence of the power spectral density at 10 Hz normalized to the applied voltage (left axis). Right axis represents the magnetoresistance vs. the magnetic field.

We have measured the $1/f$ noise resulting from the resistance fluctuations of a film of perovskite-type manganese oxide $\text{La}_{2/3}\text{Sr}_{1/3}\text{MnO}_3$ in the vicinity of the metal-insulator transition (300 K) in fields up to 27 T. Plotted in Figure 1 is the magnetic field dependence of the normalized noise level at 10 Hz (on the left axis) and the magnetoresistance (on the right axis). Whereas the magnetoresistance shows a monotonic decrease with no evidence of saturation, the noise level decreases sharply by roughly an order of magnitude between 0 and 3 T and seems to reach a baseline with no significant variations up to 27 T. These results show that the $1/f$ noise in $\text{La}_{2/3}\text{Sr}_{1/3}\text{MnO}_3$ does not probe the main conduction mechanism responsible for the nonsaturating magnetoresistance. We speculate that in this particular case the $1/f$ noise originates mainly from magnetic domain fluctuations that vanish when the sample is fully magnetized.

¹ Coey, J.M.D., *et al.*, *Adv. Phys.*, **48**, 167-293 (1998).

² Gor'kov, L.P., *et al.*, *J. Supercond.*, **12**, 243-246 (1999).

³ Fäth M., *et al.*, *Science*, **285**, 1540-1542 (1999).

High Field ESR Study of Polymeric Phases in $\text{Na}_2\text{Rb}_{1-x}\text{Cs}_x\text{C}_{60}$

Arcon, D., Univ. of Sussex, United Kingdom, Chemistry, Physics and Environmental Sciences, and J. Stefan Institute, Jamova, Slovenia

Prassides, K., Univ. of Sussex, United Kingdom, Chemistry, Physics and Environmental Sciences, and J. Stefan Institute, Jamova, Slovenia

Maniero, A.L., NHMFL

Brunel, L.-C., NHMFL

$\text{Na}_2\text{RbC}_{60}$ was shown to polymerise below about 250 K if the material is subjected to extremely slow cooling. Structural studies have confirmed the occurrence of polymerisation for the entire $\text{Na}_2\text{Rb}_{1-x}\text{Cs}_x\text{C}_{60}$ family at both ambient and elevated pressure. Both monomeric pc and monoclinic polymeric phases coexist below 250 K with the amount of the polymeric phase strongly depending on x as well as on cooling rate.

The polymerization of C_{60}^{3-} ions in $\text{Na}_2\text{RbC}_{60}$ is characterized by a different structural motif than that encountered in the extensively studied RbC_{60} polymer phase, involving a single C-C bridging bond. As a result, the C_{60} - C_{60} intrachain distance (~ 9.35 Å) in $\text{Na}_2\text{RbC}_{60}$ is longer than that in RbC_{60} (~ 9.11 Å).

Å). It is in fact comparable with the C_{60} - C_{60} interchain distance, which in Na_2RbC_{60} amounts to 9.966 Å. A quasi-one-dimensional electronic structure for the Na_2RbC_{60} phase is thus somehow unlikely. Partial replacement of Rb by Cs to give $Na_2Rb_{1-x}Cs_xC_{60}$ ($0 \leq x \leq 1$) allows the formation at ambient or elevated pressure of a family of isostructural polymer phases in which the chain-chain separation can be controlled. For instance, the C_{60} - C_{60} interchain distance increases by $\sim 0.22\%$ from 9.966 Å in Na_2RbC_{60} to 9.988 Å in $Na_2Rb_{0.3}Cs_{0.7}C_{60}$ at 200 K. The question of how this expansion of the chain-chain distance may affect the electronic and magnetic properties of the polymer phases in $Na_2Rb_{1-x}Cs_xC_{60}$ was a subject of a research project applying the high field ESR technique.

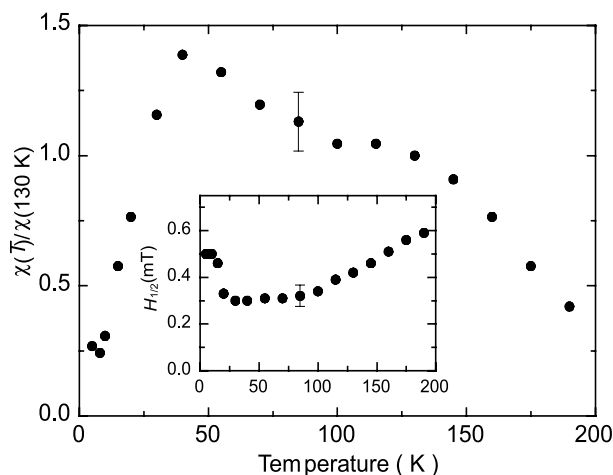


Figure 1. Temperature dependence of the ESR susceptibility and homogeneous linewidth (inset) in $Na_2Rb_{0.3}Cs_{0.7}C_{60}$ at $\nu_L = 109.056$ GHz.

We found that the magnetic properties of the low-temperature polymer phases in $Na_2Rb_{1-x}Cs_xC_{60}$ at 110 GHz microwave frequency with x varying between 0 and 1 strongly depend on the Cs content and its electronic structure progressively becomes quasi-one-dimensional as x is increased. While the electronic properties of polymeric Na_2RbC_{60} are close to those of a three-dimensional metal, $Na_2Rb_{0.3}Cs_{0.7}C_{60}$ shows characteristics of quasi-one-dimensional metal with an instability in the electronic structure detected by the sudden disappearance of the ESR intensity due to the opening of the gap at the Fermi surface (Figure 1). The observation of an additional resonance line below 15 K, attributed to antiferromagnetic resonance, suggests that the low temperature polymeric phase in $Na_2Rb_{0.3}Cs_{0.7}C_{60}$ has a well-defined magnetic ground state.

Phase Transition in Magnetic Field in V_2O_3

Bao, W., LANL

Lacerda, A.H., NHMFL/LANL

Thompson, J.D., LANL

Rich types of phase transitions have been found and extensively studied in the Mott system V_2O_3 by doping and by applying high pressure. In this three-day work using the 20 T magnet at NHMFL/LANL, we initiated a study on the phases transitions

under high magnetic field. The stoichiometric V_2O_3 sample we used undergoes a first-order concomitant metal-insulator, antiferromagnetic and structural transition at about 150 K at ambient condition. The hysteresis loops at various magnetic field are summarized in the figure. In view of the value of the transition temperature, it may not be surprising that the 150 K transition is little affected by a magnetic field up to 18 T.

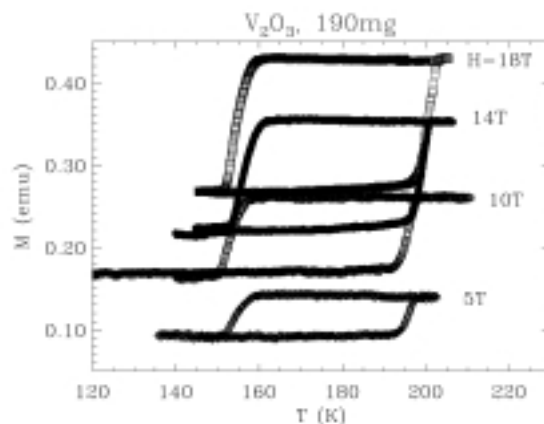


Figure 1. Magnetization as a function of temperature measured with $H = 5, 10, 14$, and 18 T.

It is planned in the next step to study a doped sample showing a second-order spin-density-wave transition at 9 K. A 20 T field should make a significant change to this low temperature phase transition.

High Field Magnetization Studies of Molecular Magnets $\{Mo_{72}Fe_{30}\}$ and $\{V_6\}$

Bud'ko, S.L., Ames Laboratory and Iowa State Univ.,
Physics and Astronomy

Canfield, P.C., Ames Laboratory and Iowa State Univ.,
Physics and Astronomy

Luban, M., Ames Laboratory and Iowa State Univ., Physics
and Astronomy

Lacerda, A.H., NHMFL/LANL

Torikachvili, M.S., San Diego State Univ., Physics

Müller, A., Universität Bielefeld, Germany, Chemistry

Kögerler, P., Universität Bielefeld, Germany, Chemistry

The paramagnetic molecular complex $\{Mo_{72}Fe_{30}\}$ has a molecular weight of approximately 18,000 and it contains 30 Fe^{+3} ions (individual spins $5/2$) situated at the 30 vertices of an icosidodecahedron.¹ These ions interact via nearest-neighbor, isotropic antiferromagnetic Heisenberg exchange. This is by far the largest molecular paramagnet that has been synthesized to date. All Fe sites in a complex are equivalent and each site has four nearest neighbors. Inter-complex interactions appear to be completely negligible in the temperature range above 2 K due to the large inter-complex spacing in a bulk sample. Because of the high spin of the individual Fe ions, the predicted² magnetic susceptibility of the classical Heisenberg model accurately

reproduces the measured susceptibility data at 0.5 T over the temperature range 1.9 to 300 K. This model also predicts frustrated magnetic ordering at low temperatures.

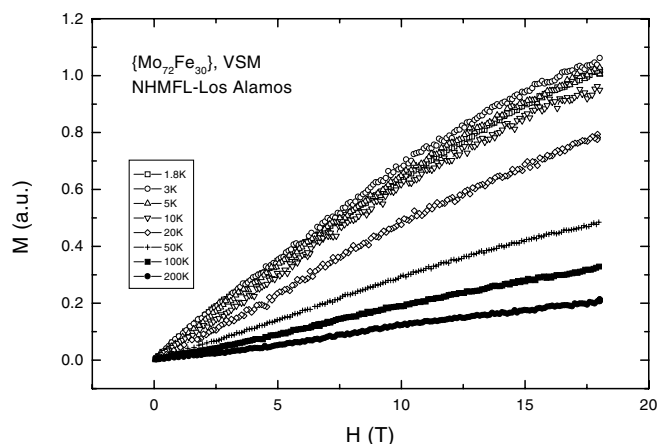


Figure 1. Field dependent magnetization of $\{\text{Mo}_{72}\text{Fe}_{30}\}$.

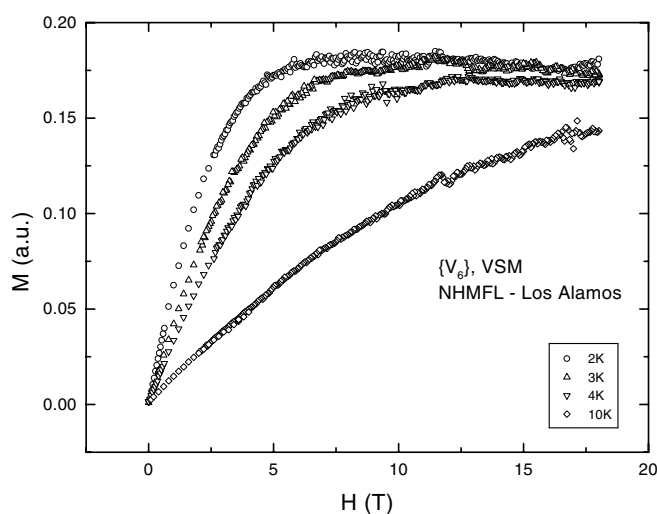


Figure 2. Field dependent magnetization of $\{\text{V}_6\}$.

We have measured the magnetic moment $M(H,T)$ versus external magnetic fields H up to 18 T for several fixed low temperatures (Figure 1). Our results will be compared to the theoretical results based on the classical Heisenberg model.

The $\{\text{V}_6\}$ compounds studied can be viewed as independent organic complexes each containing two weakly coupled near-equilateral triangles³ with one paramagnetic V^{4+} ion (spin 1/2) attached to each vertex of the triangle. Theoretical calculations⁴ based on the quantum Heisenberg model for antiferromagnetic exchange interaction between the three ion spins lead to the prediction that at fixed low temperatures T (approximately 2 K and below), the magnetic moment $M(H,T)$ per triangle versus external magnetic field H will exhibit two plateaus, of heights $1\mu_B$ and $3\mu_B$, respectively, separated by a sharp transition for a transition field $H_c \approx 50$ T. The plateaus and the sharp transition are the direct result of the ground state-first excited state level crossing associated with total spins 1/2 and 3/2. Our measurements of $M(H,T)$ for $H < 18$ T (Figure 2) have confirmed the existence of the first plateau. Future measurements that will proceed up to 60 T, will explore the

existence of the sharp transition to the second plateau. Analysis of the details of this transition will provide useful information concerning the numerical values of the exchange constants between individual pairs of V^{4+} ions.

- ¹ Müller, A., *et al.*, *Angew. Chem. Int. Ed.*, **38**, 3238 (1999).
- ² Luban, M., *et al.*, (in preparation).
- ³ Müller, A., *et al.*, *Chem. Eur. J.*, **4**, 1388 (1998).
- ⁴ Luban, M., *et al.*, (in preparation).

Magnetotransport and Quantum Oscillations in CeAgSb_2 and LaAgSb_2

Bud'ko, S.L., Ames Laboratory and Iowa State Univ.,
Physics and Astronomy

Myers, K.D., Ames Laboratory and Iowa State Univ.,
Physics and Astronomy

Canfield, P.C., Ames Laboratory and Iowa State Univ.,
Physics and Astronomy

Lacerda, A.H., NHMFL/LANL

Recent studies of anisotropic transport and magnetic properties of the RAgSb_2 ($\text{R}=\text{Y}$, La - Nd , Sm , Gd - Tm) high quality single crystals¹ have shown these materials to manifest rich and complex physical properties, including metamagnetism and large, near-linear magnetoresistance. CeAgSb_2 was characterized as a quite rare case of a moderate heavy fermion compound with ferromagnetic ordering at $T = 9.6$ K. LaAgSb_2 serves as a "reference material" for the RAgSb_2 compounds with R -magnetic rare earth, in addition a density-wave-like feature was observed in temperature dependent resistivity at $T^* = 12$ K. De Haas - van Alphen effect was detected in LaAgSb_2 in moderate applied field $H = 5.5$ T.

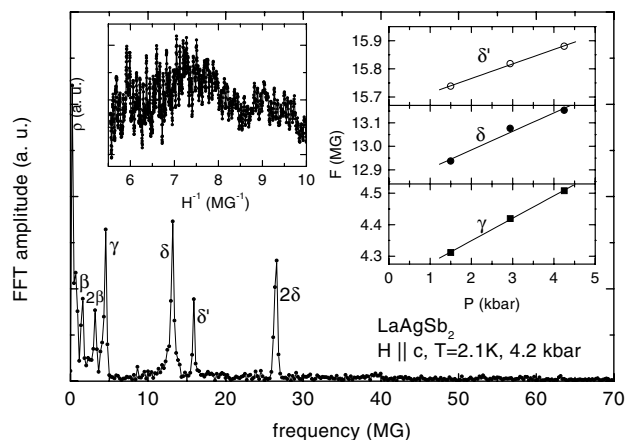


Figure 1. Fourier spectrum of Shubnikov - de Haas oscillations in LaAgSb_2 at 4.2 kbar and 2.1 K. Left inset: resistivity as a function of inverse field. Right inset: pressure dependence of the observed oscillations.

Here we briefly report the results of magnetotransport measurements on LaAgSb_2 and CeAgSb_2 under multi-extreme conditions of low temperatures ($T = 1.8$ K), hydrostatic pressure ($P = 10$ kbar) and high magnetic field ($H = 18$ T).

were performed in Oxford Instruments cryostat with VTI and 18/20 T superconducting magnet using non-magnetic Be-Cu piston-cylinder pressure cell² with a light mineral oil as a pressure media.

In LaAgSb₂ Shubnikov - de Haas oscillations from several different branches of the Fermi surface, consistent with the measured at P=0 de Haas - van Alphen frequencies, were observed. Applied pressure causes increase of the cross-section of the observed orbits (Figure 1). T* decreases under pressure with dT*/dP -4.6K/kbar. This decrease is possibly caused by diminution of the anisotropy if LaAgSb₂ under pressure. Close-to-linear field dependence of magnetoresistance persists up to 18 T.

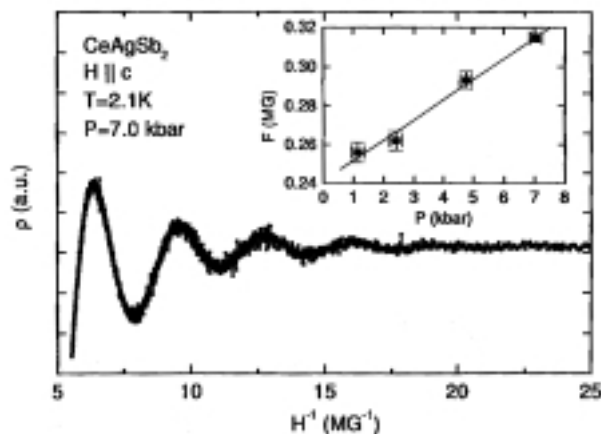


Figure 2. Shubnikov - de Haas oscillations in CeAgSb₂ at 7.0 kbar and 2.1 K (background magnetoresistance has been subtracted). Inset: pressure dependence of SdH oscillation.

In CeAgSb₂ the magnetic ordering temperature decreases under pressure with the derivative dT_C/dP -0.12K/kbar. Only a single branch of the Fermi surface with an extremely low frequency (F 0.2 5 MG at P=1.2 kbar) was observed in this compound. This frequency increases linearly with pressure with a slope of 0.01 MG/kbar (Figure 2). Although the quality of the CeAgSb₂ single crystals was comparable with LaAgSb₂ and other members of the series, CeAgSb₂ displays strong electron correlations, manifesting themselves in temperature dependent resistivity typical of a Kondo lattice, and complex ferromagnetism (with a possible conical structure). These features suggest that the Fermi surface of CeAgSb₂ may be substantially different from the other compounds.

¹ Myers, K.D., *et al.*, J. Magn. Magn. Mat., **205**, 27 (1999).

² Pressure cell was designed and built by Prof. J. Kamarad and was funded by NSF (collaborative project with the Czech Republic).

Magnetic Properties of the Linear Chain System Tetragonal LiCu₂O₂

Caldwell, T., NHMFL/FSU, Physics

McCall, S., NHMFL/FSU, Physics

Kuhns, P.L., NHMFL

Reyes, A.P., NHMFL

Cao, G., NHMFL

Moulton, W.G., NHMFL/FSU, Physics

Crow, J.E., NHMFL

LiCu₂O₂ can be grown in two phases, orthorhombic and tetragonal, the difference presumably depending on the cooling rate.¹ Single crystals of the tetragonal phase were grown and verified by X-ray diffraction studies on the resulting crystals. The tetragonal phase has two interacting perpendicular Cu²⁺ chains isolated from the next plane of chains by Li and Cu⁺ atoms (non-magnetic), in contrast to the orthorhombic phase that has two parallel interacting chains forming a conventional spin ladder. As far as we can determine these represent the first studies of the tetragonal phase and of perpendicular interacting spin chains. The magnetization is quite anisotropic and deviates appreciably from the Bonner-Fisher behavior with a broad peak at about 30 K, in contrast to about 45 K in the orthorhombic phase. The magnetization also shows an anisotropic phase transition, suggestive of long range antiferromagnetic order, near 9 K. The specific heat shows a small broad peak at 24 K with an entropy loss of about 0.6 J/mole K. A second very large,

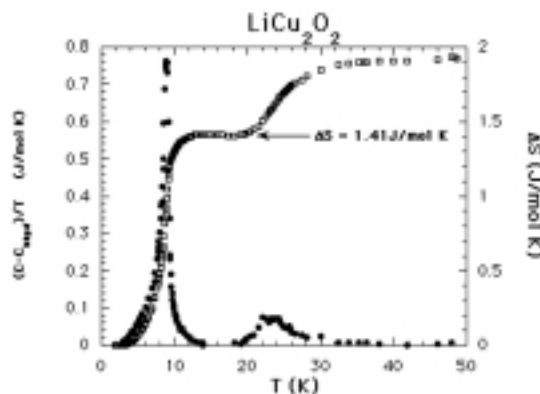


Figure 1. Specific heat and entropy change of the tetragonal phase of LiCu₂O₂ as a function of temperature. The phonon contribution has been subtracted out.

very sharp peak, with an entropy loss of about 1.4 J/mole K, appears at about 9 K, suggestive of a first order phase transition. Furthermore, the specific heat data are field independent, again suggesting a first order phase transition. ⁷Li NMR studies at 6.2 T give an e²qQ of 39*10⁻²⁸ J in the paramagnetic state. For reasons not currently understood, only the ^{63,65}Cu⁺ (non-magnetic) NMR was observed. Below 9.0 K the ⁷Li central quadrupole transition splits into 2 components, characteristic of an antiferromagnet. The splitting of 0.09 T is very unusual in the sense that it is temperature independent down to 2 K in contrast to the usual behavior of an antiferromagnet in

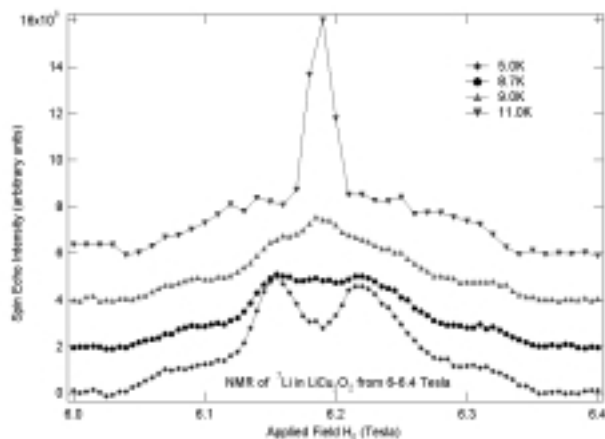


Figure 2. ^7Li NMR spectrum at temperatures close to the long range ordering, both above and below the transition, showing the splitting at the transition. The 0.09 T splitting is temperature independent down to 2 K.

which the splitting increases as the order parameter increases, since the internal field is proportional to the order parameter through the hyperfine interaction. Preliminary angle dependent studies suggest the ordered phase is a simple two sublattice antiferromagnet. Our only interpretation of these data is that the order parameter is independent of temperature, as would be the case for a first order magnetic phase transition. It is thus concluded that the tetragonal phase of LiCu_2O_2 is one of the very rare examples of a first order antiferromagnetic phase transition.

¹ Vorotynov, *et al.*, J. Exp. Theor. Physics, **86**, 1020 (1998).

Impact of Dilute La-Doping on Metal-Insulator Transition and Magnetic Phase Transition in Ca_2RuO_4 **IHRP**

Cao, G., NHMFL
McCall, S., NHMFL
Dobrosavljevic, V., NHMFL
Alexander, C.S., NHMFL
Crow, J.E., NHMFL
Guertin, R.P., Tufts Univ., Physics

Ca_2RuO_4 is a Mott system with a structurally driven metal-insulator transition at $T_{\text{MI}}=357$ K and a Néel temperature at $T_{\text{N}}=110$ K. Slight substitution of trivalent La for divalent Ca in Ca_2RuO_4 drastically reduces T_{MI} and the electrical resistivity (see Figure 1), simultaneously precipitating robust ferromagnetism (FM) in the antiferromagnetic (AFM) host (see Figure 2). T_{c} is conspicuously and consistently lower than T_{MI} , suggesting that the metal-insulator transition is not driven by the magnetic instability. The La substitution also results in a rapid increase in both the Pauli susceptibility and electronic specific heat coefficient, and a crossover from hopping conductivity

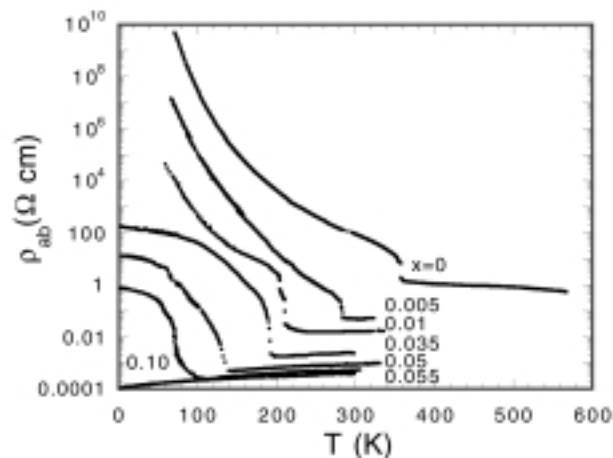


Figure 1. Resistivity $\rho(T)$ for basal plane as a function of temperature T for single crystal $(\text{Ca}_{1-x}\text{La}_x)_2\text{RuO}_4$.

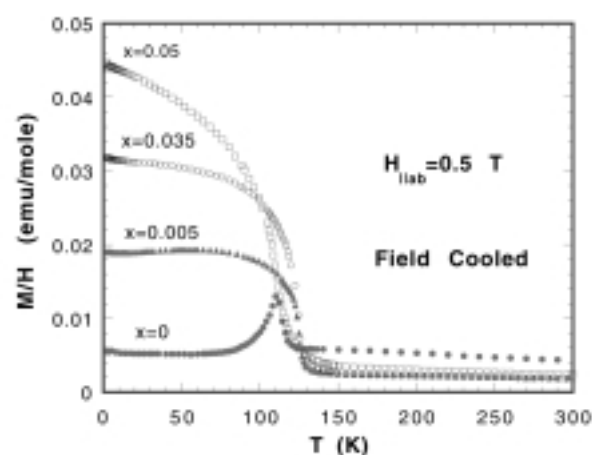


Figure 2. Magnetic susceptibility M/H for basal plane as a function of temperature T for single crystal $(\text{Ca}_{1-x}\text{La}_x)_2\text{RuO}_4$.

to disordered metallic behavior at low temperatures. These dramatic changes suggest a near degeneracy of the ground state and a subtlety of competition between FM and AFM coupling in Ca_2RuO_4 .

Rapid Suppression of Metal-Insulator Transition, and Magnetic Moment for Dilute La-Doping in $\text{Ca}_3\text{Ru}_2\text{O}_7$ **IHRP**

Cao, G., NHMFL
Crow, J.E., NHMFL
Alexander, C.S., NHMFL
McCall, S., NHMFL
Guertin, R.P., Tufts Univ., Physics

$\text{Ca}_3\text{Ru}_2\text{O}_7$ is a “badly” conducting metal at high temperatures. It orders antiferromagnetically at $T_{\text{N}}=56$ K and undergoes a metal to insulator transition at T_{MI} . Both transitions can rapidly be suppressed by only slight substitution of the divalent Ca

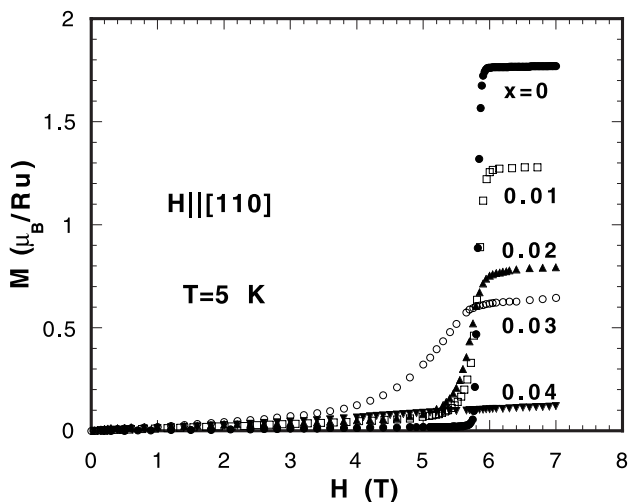


Figure 1. Magnetization M for the easy axis as a function of magnetic field, H , for single crystal $(\text{Ca}_{1-x}\text{La}_x)_3\text{Ru}_2\text{O}_7$.

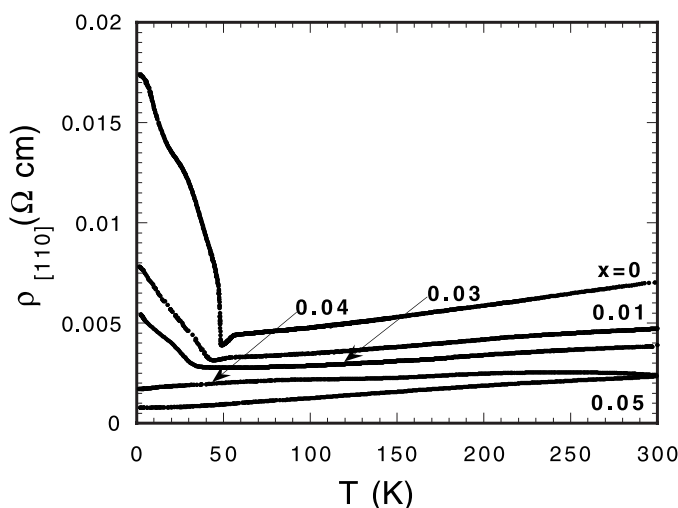


Figure 2. Resistivity $\rho(T)$ for the easy axis as a function of temperature, T , for single crystal $(\text{Ca}_{1-x}\text{La}_x)_3\text{Ru}_2\text{O}_7$.

by the trivalent La. For as little as 5 percent La ($x=0.05$) in $(\text{Ca}_{1-x}\text{La}_x)_3\text{Ru}_2\text{O}_7$ the magnetic moment ($1.7 \mu_B/\text{Ru}$) is fully quenched (Figure 1) and the electrical resistivity remains metallic down to $T=0$ K (see Figure 2). This rapid suppression is reflected in the quenching of field-induced transitions for $0 < H < 20$ T and $0 < T < T_N$ along the “easy axis.” In addition, the large negative magnetoresistance always exhibits unusually large hysteresis. The magnetic moment suppression accompanying the approach to the metallic ground state demonstrates persuasively that the spin and charge degrees of freedom are strongly coupled and that the d-electrons serve a dual function—to produce the localized moment on the Ru site and to serve as carriers for the electrical conductivity.

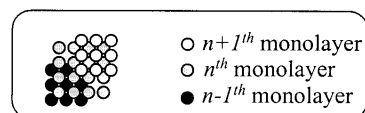
“Quasi 2-D” Spin Distributions in II-VI Magnetic Semiconductor Heterostructures: Clustering and Dimensionality

Crooker, S.A., NHMFL/Los Alamos

Samarth, N., Pennsylvania State Univ., Physics

Awschalom, D.D., Univ. of California at Santa Barbara, Physics

Spin clustering is ubiquitous in II-VI diluted magnetic semiconductors (DMS). Clear predictions can be made for the number and type of spin clusters in 3D systems (e.g., bulk $\text{Cd}_{1-x}\text{Mn}_x\text{Se}$), where the distribution of magnetic Mn^{2+} cations is random and isotropic. In 2D, spin clustering (arising mainly from an antiferromagnetic exchange between neighboring magnetic cations) should be greatly reduced, leading to enhanced paramagnetism. However, perfect 2D interfaces and monolayers are never actually realized due to the inevitable inter-monolayer mixing of atoms during MBE growth, which smears the magnetic cations over several monolayers. Common mechanisms include segregation (mixing between the monolayer being grown and the underlying monolayer) which leads to roughly exponential magnetic profiles, and diffusion (which can arise from, e.g., high growth temperatures or annealing) which leads to gaussian profiles. Hence, real DMS heterostructures contain “quasi-2D” distributions of spins, with a corresponding magnetization and degree of spin clustering somewhere between that of bulk (3D) and planar (2D) spin distributions.



Singles: $y_n^4 y_{n+1}^4 y_{n-1}^4$ (where $y_n = 1 - x_n$)

Pairs: $4x_n y_n^6 y_{n+1}^6 y_{n-1}^6 + 4x_{n+1} y_n^5 y_{n-1}^5 y_{n+2}^4 + 4x_{n-1} y_n^5 y_{n+1}^4 y_{n-2}^5$

Closed triples: $4x_{n+1}^2 y_{n-1}^4 y_n^6 y_{n+1}^6 y_{n+2}^6 + 4x_{n-1}^2 y_{n+1}^4 y_n^6 y_{n-1}^6 y_{n-2}^6 + 8x_n x_{n+1} y_{n-1}^6 y_n^6 y_{n+1}^4 y_{n+2}^4 + 8x_n x_{n-1} y_{n+1}^6 y_n^6 y_{n-1}^4 y_{n-2}^4$

Open triples: $6x_n^2 y_n^8 y_{n+1}^8 y_{n-1}^8 + 12x_n^2 y_n^7 y_{n+1}^8 y_{n-1}^8 + \dots$

Figure 1. The probability of clustering for a spin in the n^{th} (100) monolayer of an arbitrary Mn distribution.

It is desirable to quantitatively predict the degree of this spin clustering in a given DMS heterostructure so that accurate comparisons can be made with real data. We determine exact expressions for computing the number and type of spin clusters (singles, pairs, open- and closed triples) for arbitrary

distributions of magnetic spins in the common (100) growth direction. The results reveal a rather surprising insensitivity of the computed magnetization to the form of the intermixing profile (exponential/gaussian), and highlight limits on the maximum possible magnetization using MBE techniques.¹

Figure 1 shows the probability of magnetic cation belonging to a single, pair, or open- and closed-triple. Single Mn^{2+} cations with no magnetic NNs are $S=5/2$ paramagnets, with Brillouin-like magnetization. Two neighboring Mn^{2+} cations form an antiferromagnetically-locked pair with zero spin at low magnetic fields, and step-like magnetization at high fields and low temperatures. Three Mn^{2+} spins can form a closed or open triple with net spin $S_T=1/2$ and $S_T=5/2$ (respectively) at low fields, and a unique set of magnetization steps at high fields.

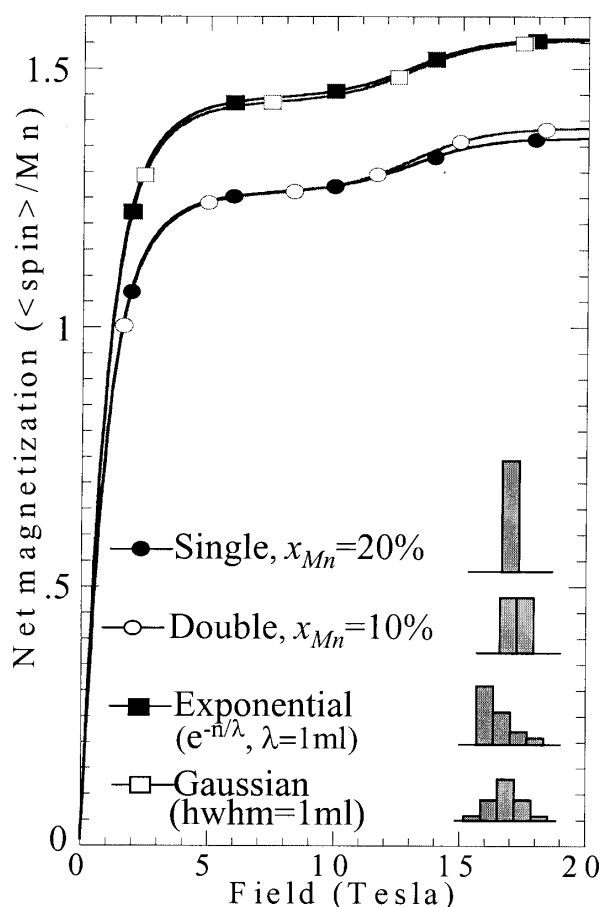


Figure 2. Calculated magnetizations in the quasi-2D profiles shown. Despite very different intermixing profiles, the magnetization is often indistinguishable.

Figure 2a shows the calculated magnetization from the profiles shown. Though unrealistic, the first two profiles—a perfect 2D plane with $x_{\text{Mn}}=20\%$ and two adjacent planes with $x_{\text{Mn}}=10\%$ —illustrate an important point: clustering often “conspires” to equalize low-field magnetizations. Although the single monolayer contains 5% fewer single Mn^{2+} spins, it contains over a third *more* open triples and higher-order clusters, which act to equalize the deficit. Only at the first magnetization step are the profiles distinguishable, as the single monolayer

contains fewer Mn-Mn pairs. The last two profiles represent the exponential and gaussian profiles roughly expected from segregation and diffusion, with decay length and half-width equal to 1 ml. Again, the calculated magnetizations are nearly identical. Thus, magnetization measurements alone cannot distinguish the form of the spin profile. However, *assuming* a particular form, the magnetization does depend sensitively on the segregation (or diffusion) length, which can then be used to fit an intermixing lengthscale in real data.

¹ Crooker, S. A., *et al.*, Phys. Rev. B, **61**, in press (Jan. 15, 2000).

A Study of the Magneto-Electronic Properties of Novel Semiconducting and Semimetallic Structures

Datta, T., Univ. of South Carolina, Physics and Astronomy
Bleiweiss, M., Univ. of South Carolina, Physics and Astronomy

We are currently studying the interaction between magnetic fields and transport electrons in a number of solid materials, in particular, magnetoresistance (MR) and Shubnikov-de Haas (SdH) oscillations. The two primary materials of interest are $\text{La}_{1-x}\text{A}_x\text{MnO}_3$ (where A is either Ca or Sr) perovskite thin films grown by an electrodeposition technique and a synthetic opal structure that has been pressure infiltrated with bismuth.

The manganate perovskites have the interesting property that they exhibit an extremely large negative MR, termed colossal magnetoresistance (CMR). This phenomenon has attracted a great deal of attention in the past several years due to the possible technological applications, as well as providing insight into exactly how magnetic fields interact with the transport electrons in these solids. The CMR effect typically occurs in the region near the Curie temperature where the material undergoes a magnetic phase transition from a paramagnetic to ferromagnetic state. That is, a change in the conductivity from insulator to metal accompanies the change in magnetic ordering; so that the magnetically disordered state is associated with insulating or semiconducting transport and the magnetically ordered ferromagnetic phase is associated with metallic conduction. This type of metal-insulator transition is unusual and poorly understood. Several theories attempting to explain CMR have been proposed and account for some aspects of CMR, but they are, at the very least, incomplete.¹ Further study is needed to determine which of these models, if any, is better in explaining the mechanism for CMR.

The manganate samples used were grown on several different metallic substrates, including iron and silver, via electrodeposition. This process causes grain boundaries and grain sizes that differ from those grown by other more standard techniques. These parameters are believed to play an essential role in determining the strength of the CMR effect in at least one of the leading theories. High magnetic field

are necessary to distinguish between the mechanisms proposed to be the cause of CMR.

Another material we are studying which has interesting properties, including very large (positive) MR, is high purity bismuth infiltrated into the interstitial regions of synthetic opals. Bismuth is a well-known semimetal whose electronic properties are very different from common metals. Because of these properties, bismuth thin films have been used to study quantum effects and the influence of reduced dimensionality has been seen in samples with dimensions on the order of 100 nm.² Finite size effects in these systems have led to enhanced MR and SdH oscillations.^{3,4} SdH oscillations, like the de Haas van Alphen effect, can only be seen using high magnetic fields.

The artificial opal structures we utilize are comprised of silica spheres of uniform size in an face centered, close packed cubic lattice. This leads to regularly spaced and shaped voids between the spheres of two types, tetrahedral and octahedral. They have approximate sizes on the order of 100 nm for the tetrahedral voids and 35 nm for the octahedral ones. Filling these voids provides a regular, three dimensional structure composed of nanoscale regions.

¹ Matl, P., *et al.*, Phys. Rev. B, **57**, 10248 (1998).

² Heremans, J., *et al.*, Phys. Rev. B, **58**, R10091 (1998).

³ Liu, K., *et al.*, Phys. Rev. B, **58**, R14681 (1998).

⁴ Zhang, Z., *et al.*, Appl. Phys. Lett., **73**, 1589 (1998).

High Frequency Resonant Experiments in the Nanomagnet Fe₈: Evidence for Coherent Magnetization Tunneling

Del Barco, E., Universitat Barcelona, Departament de Física Fonamental

Hernandez, J.M., Universitat Barcelona, Departament de Física Fonamental

Tejada, J., Universitat Barcelona, Departament de Física Fonamental

Biskup, N., NHMFL

Achey, R., NHMFL

Rutel, I., NHMFL

Dalal, N., NHMFL/FSU, Chemistry

Brooks, J.S., NHMFL/FSU, Physics

Fe₈ (an abbreviation for [(C₆H₁₅N₃)₆Fe₈ (μ₃-O)₂(μ₂-OH)₁₂(Br₇(H₂O))Br₈H₂O] is a magnetic molecule with spin $S = 10$ with (at low temperatures) constant magnetic moment $m = 20\mu_B$. Due to this “nanomagnetism,” such materials opened a new area in the investigation of macroscopic quantum mechanical phenomena. We performed an extensive investigation of resonant phenomena arising from coherent quantum tunneling. We used a resonant cavity method to probe a wide number of transitions between quantum states

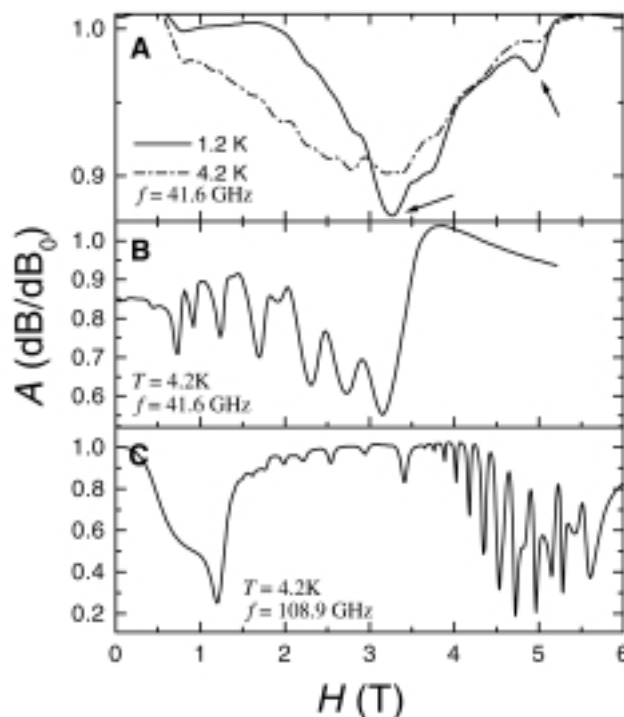


Figure 1. Normalized signal amplitude (A) vs. magnetic field (H) for (a) oriented powder and (b-c) single crystal.

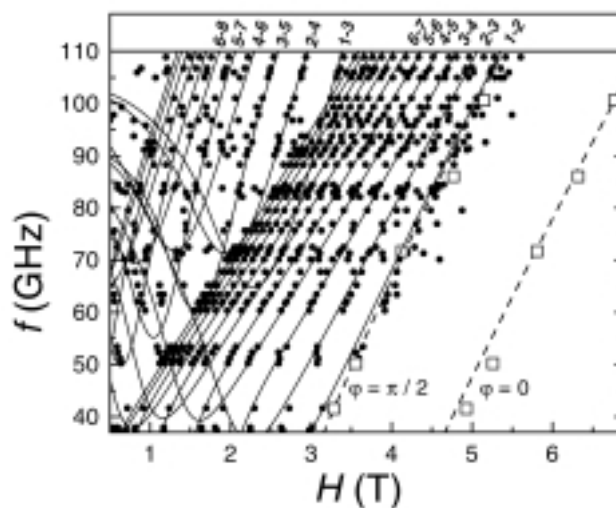


Figure 2. Resonant frequency (f) as a function of the field (H). Solid circles: single crystal. Open squares: oriented powder.

with magnetic field perpendicular to the easy axis. Resonant absorptions at 40 different frequencies (37-110 GHz) were detected by a millimeter wave network analyzer (MVNA). In Figure 1 we show an example of these absorptions in (a) an oriented powder at 41.6 GHz, and (b-c) a single crystal for two different frequencies. The two assigned peaks in (a) correspond to coherent tunneling between $S_z = \pm 10$ levels. They are visible (most pronounced) at lowest temperature (1.2 K) when the population of the higher levels is negligible. Due to the random orientation of the hard axis in the magnetic field, only the parallel and perpendicular components prevail and give two peaks. In the single crystal at higher temperatures (4.2 K) a whole set of absorption lines indicate transitions between consecutive magnetization levels and their quantum splittings.

In Figure 2 we plot transitions for 40 different frequencies. Solid lines are theoretical predictions after diagonalizing the Hamiltonian:

$$H = -DS_z^2 + ES_z^2 - g\mu_B \vec{H} \vec{S}$$

This shows remarkable agreement between experimental and theoretical results.

High Field Magnetotransport Measurements in Perovskites Compounds

Gama, S., UNICAMP, Campinas, Brazil

Coelho, A.A., UNICAMP, Campinas, Brazil

Rivas-Padilla, E.P., UNICAMP, Campinas, Brazil

The material of interest for these measurements were manganite ceramics of the perovskite structure presenting magnetoresistive effects. All samples were prepared by solid state reaction-sintering procedure.

Resistivity measurements as a function of temperature and applied magnetic field down to 2.5 K were performed.

Three set of samples have been measured. The first one comprises four samples with constant variance in the A site radii distribution at a value of 0.0015 Å², and average A radii varying from 1.2245 up to 1.2337 Å. The second set comprises four samples with constant variance of 0.0072 Å², with A radii varying from 1.2271 Å up to 1.2321 Å. Finally, the third set comprises six samples of base composition La_{0.67}Sr_{0.33}MnO₃ doped with the rare-earth Er and Gd.

For the first two sets of samples the objective is to study the effect of size variation at the site A at constant variance on the transport and magnetic properties of these materials. For the third set of samples the objective is to investigate the effect of rare earth doping in the transport and magnetic properties of the base material. The obtained preliminary results show a very consistent evolution of the magnetotransport properties with the constant variance (A) and the rare-earth concentration.

Electronic Properties of Doped Manganites

Gor'kov, L.P., NHMFL

Dzero, M.O., NHMFL

Kresin, V.Z., Lawrence Berkeley National Laboratory

As continuation of our studies of doped (pseudo-cubic) manganites, A_{1-x}B_xMnO₃,^[1] the efforts have now been concentrated along two directions.

I. Percolative transition in manganites as a new type of metal-insulator transition. In more general terms, the problem concerns

properties of heavy doped transition metal oxide and is akin to physics in doped superconducting cuprates where the possibility of electronic phase separation, heterogeneity introduced by the Coulomb forces are also expected to lead to the percolative features in doping dependence of the physical characteristics.² Consequences of this notion if applied to manganites are discussed in References 3 and 4. Recent experimental data⁵ provides strong support to these views.⁶

II. Sharp increase in content of the conducting (and ferromagnetic) fraction in manganites at concentrations where the "colossal magnetoresistance" is optimal (i.e., at x~0.3 - 0.4) makes it possible to describe the low temperature properties in terms of a Fermi-liquid like two band model.^{3,4} Among other findings, it is shown that the "2.5"-topological ("Lifshitz") transition occurs at x=0.3, as seen from a "neck" formation on the calculated Fermi-surfaces. Analysis of the resistivity data leads to the conclusion that while dependence of the tolerance factor on the "average" structure makes no big impact on the bandwidth, its local variation, i.e., local mismatches in the radii of ions A and B, determines how close lies the Fermi level in a specific material to the Anderson's mobility edge.^{3,4}

¹ Gor'kov, L.P. *et al.*, NHMFL Ann. Report 1999.

² Gor'kov, L.P., JETP Lett., **46**, 420 (1987).

³ Dzero, M.O. *et al.*, Solid State Commun., **112**, 707 (1999).

⁴ Dzero, M.O. *et al.*, Europhys. Journ. (1999, accepted).

⁵ Fath, M., *et al.*, Science **285**, 1540 (1999).

⁶ Gor'kov, L.P. *et al.*, J. Superconductivity (1999, accepted).

Search for High Field-Induced Magnetic Transitions in Ca₃Ru₂O₇ and BaIrO₃

Guertin, R.P., Tufts Univ., Physics

Harrison, N., NHMFL/LANL

Cao, G., NHMFL

Crow, J.E., NHMFL

Ca₃Ru₂O₇ and BaIrO₃ have perovskite-derived layered structures, BaIrO₃, being quasi-one dimensional, and both have long range magnetic order, at T_N = 56 K and T_C = 175 K, respectively. For BaIrO₃ this is surprising because the magnetic moments is only about 0.03 mB/Ir, far below 1.0 mB/Ir expected for its valence and configuration.

Of all the Ruddlesden-Popper series ruthenates, Ca₃Ru₂O₇ has the richest array of transport and magnetic transitions, featuring a metal insulator transition at 48 K. We successfully measured M(H) at T = 4 K and at several temperatures up to 50 K and in fields up to 55 T. This was the first stabilization of the cryostat to high temperatures, as it is normally used for very low temperature (T<1 K) dHvA or SDH measurements. The orientation of the field was along the a and b-axis in this orthorhombic structure material. We found the expected 6 T metamagnetic transition along the a-axis, and most importantly, no further transitions up to 55 T, confirming lower field measurements. Along the b-axis we found two transitions, at

T and 19 T and none higher. The 14 T is not understood, but the 19 T transition extrapolates well from dc data.

The aim of the BaIrO₃ measurements was to determine if any high field metamagnetic transitions were present, but none were found up to 55 T, even though the temperature was scanned to above T_C¹. BaIrO₃ has been called a canted antiferromagnet, explaining the very small magnetic moment. However, sufficiently high fields should uncouple the Ir moments yielding a full moment, particularly near T_C². The results confirmed that the magnetically ordered iridates have intrinsically low moments. This is not well understood, though it calls to mind recent work in the doped hexaborides which show a very high TC but with minuscule magnetic moment, this being attributed to a dilute interacting electron gas.

A final experiment was carried out in collaboration with the R. Clark group from Univ. of New South Wales. This was to test a new probe for M(t) measurements that incorporated lithographed pickup coil circuitry. A Ca₃Ru₂O₇ sample oriented with H||a and H||b was tested, and the expected 6 T transition was found, with exceptional signal to noise. For H||b we found the transitions alluded to above. It is not necessary to perform sample, in vs. out, procedures with this probe; the coils are perfectly balanced through lithographic techniques. These were the first non-dHvA tests run on the new probe, demonstrating its use for pulsed field magnetization experiments.

¹ Cao, G., *et al.*, to be published in Solid State Commun.

² Lindsay, R., *et al.*, Solid State Commun., **86**, 759 (1993).

Spin-Peierls Transition in NaV₂O₅ at High Magnetic Fields **IHRP**

Hebard, A.F., UF, Physics/NHMFL

Bompadre, S.G., UF, Physics/NHMFL

Kotov, V.N., UF, Physics/NHMFL

Hall, D., NHMFL

Maris, G., Univ. of Groningen, The Netherlands, Chemical Physics

Bass, J., Univ. of Groningen, The Netherlands, Chemical Physics

Palstra, T.T.M., Univ. of Groningen, The Netherlands, Chemical Physics

Recently, the inorganic compound, NaV₂O₅, was shown to behave as a spin-Peierls material with a transition temperature T_c ≅ 34 K. Lattice distortions also take place at the transition, as observed in x-ray diffraction experiments, thus revealing the intimate relation between magnetic and lattice properties. Using a metal-foil cantilever beam magnetometer we have found an anomalously weak field dependence to T_c(H) that extends to 30 T. We argue that a charge ordering transition accompanied by singlet formation is consistent with our observations.¹

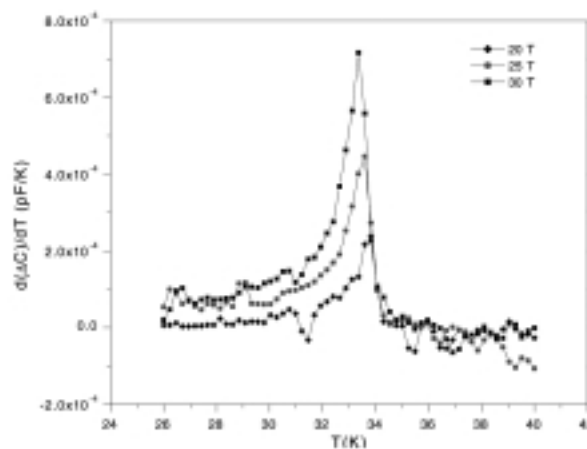


Figure 1. Temperature dependence of the derivative of the capacitance readings (proportional to magnetization) with respect to temperature at the indicated fields for a 1.9 mg single crystal sample located at field center. In the field center position the cantilever is primarily sensitive to torque.

A capacitance bridge was used to monitor the changes in force (magnetization) for temperature sweeps in fixed field. The same bare cantilever was measured under the identical conditions (sweep direction and sweep rate) as the cantilever-plus-sample combination to provide a background reference that could then be subtracted from the data. The data in all field positions scale with a quadratic dependence in field as expected from both torque and force contributions. The position of the peaks determined from the temperature-dependent cantilever measurements (see Figure 1) reveal a surprisingly weak field-dependent transition temperature T_c(H). We calculate a reduced temperature shift, ΔT_c/T_c(0), which when plotted in terms of the scaled magnetic field h = gμ_BH/2kT_c(0), has the dependence, ΔT_c/T_c(0) = -αh². A quadratic dependence is expected from theory for h ≪ 1. Our experimental value α = 0.073 signifies a very weak field dependence that is also in agreement with data obtained from specific heat measurements in fields up to 16 T.² In contrast, the “conventional” inorganic spin-Peierls compound CuGeO₃ exhibits a factor of five stronger field dependence with α = 0.39,³ a value in very good agreement with theoretical expectations for a pure spin-Peierls system uncomplicated by a simultaneously occurring charge-ordering transition.

¹ Bompadre, S.G., *et al.*, cond-mat/9911298, submitted Phys. Rev. B.

² Schnelle, W., *et al.*, Phys. Rev. B, **59**, 73 (1999).

³ Hase, M., *et al.*, Phys. Rev. B, **48**, 9616 (1995).

Melting of Charge/Orbital Ordered States in $\text{Nd}_{1/2}\text{Sr}_{1/2}\text{MnO}_3$: Magnetic Field Dependent Optical Studies

Jung, J.H., Seoul National Univ. (SNU)-Korea, Physics

Lee, H.J., SNU-Korea, Physics

Noh, T.W., SNU-Korea, Physics

Choi, E.J., Univ. of Seoul-Korea, Physics

Moritomo, Y., Nagoya Univ.-Japan, Applied Physics

Wang, Y.J., NHMFL

Wei, X., NHMFL

Doped manganites with small bandwidths near half doping show intriguing charge ordering phenomena, i.e. real space orderings of the Mn^{3+} and the Mn^{4+} ions. The charge ordering in $\text{Nd}_{1/2}\text{Sr}_{1/2}\text{MnO}_3$ incorporates $d_{3x^2-r^2}$ ($d_{3y^2-r^2}$) orbital ordering and CE-type antiferromagnetic spin ordering. Interestingly, it was found that some charge ordered states could be changed into ferromagnetic metallic states under a high magnetic field.¹ (This transition is usually called “melting” of charge/orbital ordered states.) Although it is a very intriguing phenomenon, its electrodynamics has been rarely investigated.

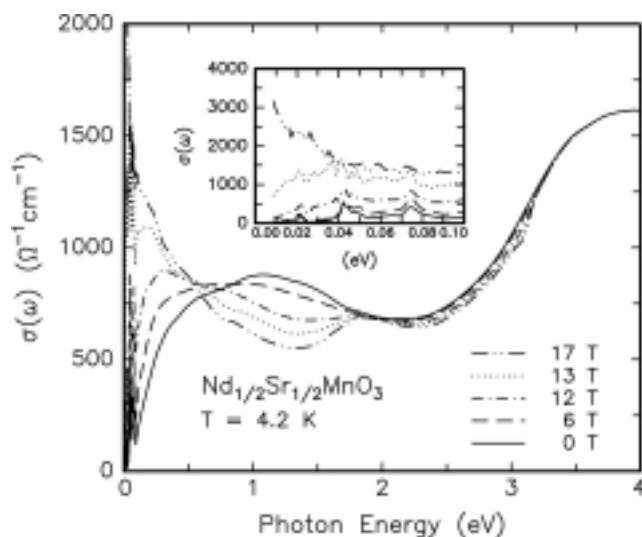


Figure 1. H-dependent $\sigma(\omega)$ of $\text{Nd}_{1/2}\text{Sr}_{1/2}\text{MnO}_3$. In the inset, $\sigma(\omega)$ below 0.1 eV are shown.

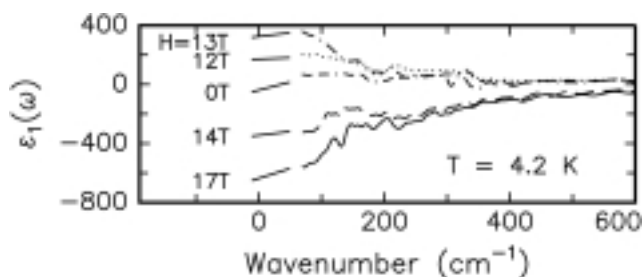


Figure 2. H-dependent ϵ_1 of $\text{Nd}_{1/2}\text{Sr}_{1/2}\text{MnO}_3$.

We measured magnetic field ($H = 0 \sim 17$ T) dependent optical conductivity spectra $\sigma(\omega)$ of $\text{Nd}_{1/2}\text{Sr}_{1/2}\text{MnO}_3$. The H-dependent $\sigma(\omega)$ at 4.2 K are shown in Figure 1. At 0 T, the spectra show typical features of a charge/orbital ordered insulator with ~ 0.1 eV optical gap. With increasing H, the spectral weights near 1.2 and 2.7 eV are transferred to lower energy regions. The gap values seem to decrease and finally disappear above 13 T. Details of transferred spectral weights below 0.1 eV can be seen in the inset of Figure 1. With increasing H, the phonon modes at 0 T are screened and the Drude peak appears above 13 T. Note that the Drude peak becomes clear and appeared below 0.04 eV. Therefore, $\sigma(\omega)$ of melted states should be viewed as two absorptions i.e., Drude weight and an incoherent peak, similar to ferromagnetic metallic states of colossal magnetoresistance manganites.²

To get a better understanding on the insulator-metal transition, we plot the real part of the dielectric constant ϵ_1 as shown in Figure 2. In the insulating state at 0 T, ϵ_1 is positive and $d\epsilon_1/d\omega > 0$. With increasing H up to 13 T, ϵ_1 increases. Above 14 T, it becomes negative and $d\epsilon_1/d\omega > 0$, which is consistent with metallic responses. To explain this intriguing behavior of ϵ_1 , we applied a composite medium model.³ The excellent agreement between the experimental data and the theoretical predictions strongly suggests that the melting of charge/orbital ordered states should occur through the percolation of ferromagnetic metal domains.

¹ Kuwahara, H., *et al.*, Science, **270**, 961 (1995).

² Kim, K.H., *et al.*, Phys. Rev. Lett., **81**, 1517 (1998).

³ Noh, T.W., *et al.*, Phys. Rev. B, **33**, 3793 (1986).

Field-Induced Magnetic Properties in the Molecule-Based Magnets: $\text{M}[\text{N}(\text{CN})_2]_2$ ($\text{M} = \text{Mn, Fe}$)

Kmety, C.R., The Ohio State Univ., Physics

Epstein, A.J., The Ohio State Univ., Physics and Chemistry

We have studied the magnetic properties of polycrystalline powders of the molecule-based magnets $\text{M}[\text{N}(\text{CN})_2]_2$ ($\text{M} = \text{Mn, Fe}$) by dc magnetization using a cantilever beam magnetometer and ac susceptibility ($T = 37$ and 45 mK, $0 \leq H \leq 18$ T), and specific heat ($1.8 \leq T \leq 50$ K, $H = 0$ and 12 T). The samples were prepared in the form of oriented powder (Mn, dc magnetization) and/or pressed pellets. In order to align the crystallites with their easy axes along the field direction, the Mn sample was mixed with Stycast 1266 and allowed to set in a magnetic field of 15 T at 298 K. Similar preparation of the Fe sample was not possible due to the reaction of the sample with the Stycast 1266. Our main goal was to detect field-induced spin rotation transitions and energy-level crossings evidenced by steps in the dc magnetization. Each magnetization step is accompanied by a peak in the ac susceptibility. Based on the temperature requirement for resolving these features, $k_B T \ll |J|$, the use of a dilution refrigerator was necessary. In addition, specific heat studies (in collaboration with S. McCall and

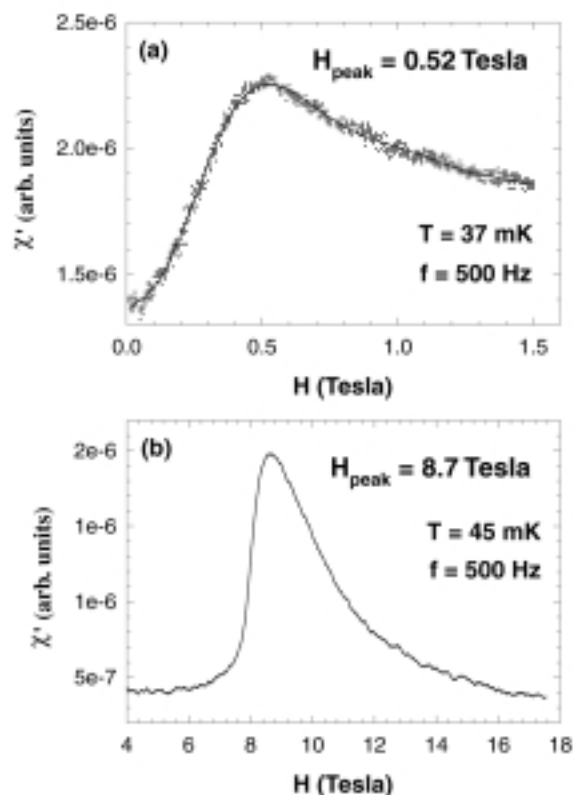


Figure 1. Real or in-phase components of the ac susceptibility as a function of temperature for $M[N(CN)_2]_2$ (a) $M = Mn$ and (b) $M = Fe$. The solid line in (a) is only a guide for the eye.

J.E. Crow from NHMFL) allowed the determination of the total magnetic entropies and energies participating in the ordering process.

Both compounds belong to the isostructural series $M[N(CN)_2]_2$ ($M = Mn, Fe, Co, Ni, Cu$). Zero-field neutron diffraction studies^{1,2} showed that the magnetic structure is noncollinear antiferromagnetic with the spin direction mainly along the a -axis for the Mn and Fe compounds, and collinear ferromagnetic with the spin direction along the c -axis for the Co and Ni compounds. The Cu compound is a ferromagnet with a transition temperature below 1.8 K (this work). For the Mn compound, field-dependent ac susceptibility ($T = 4.5$ K) and neutron diffraction ($T = 0.4, 1, 3.3$ K) measurements² revealed the occurrence of a spin rotation transition at a critical field of 0.52 T. For the Fe compound, isothermal magnetization ($T = 5$ K) measurements² indicated that $M(5.5 \text{ T}) = 5400 \text{ emu Oe/mol}$, which is much lower than the value expected for a $S = 2$ system.

The magnetic studies of the molecule-based magnets $M[N(CN)_2]_2$ ($M = Mn, Fe$) performed at the NHMFL revealed peaks in the ac susceptibilities at $H = 0.52 \text{ T}$ ($T = 37 \text{ mK}$) for the Mn compound (Figure 1(a)), and at $H = 8.5 \text{ T}$ ($T = 45 \text{ mK}$) for the Fe compound (Figure 1(b)). Also, steps in the dc magnetization may occur at $H = 11 \text{ T}$ (ramp up) and 9 T (ramp down) for the Fe compound, but the latter measurements must be repeated using a more appropriate cantilever. The results for the Mn compound are nearly identical to that of a magnetic field scan taken at 100 times higher temperature of 4.5 K at The Ohio State University. The results are also in agreement with

earlier neutron diffraction studies (performed at NIST) which showed a magnetic field dependent, temperature independent ($0.4 \leq T \leq 3.3 \text{ K}$) reduction in magnetic scattering intensity for the (001) magnetic Bragg peak. The data, taken together, demonstrate the absence of thermal barriers to spin motion in this system. The results for the Fe compound combined with previous isothermal ($T = 5 \text{ K}$) magnetization studies at The Ohio State University suggest that a crossing of the energy levels $|S_z = 1\rangle$ and $|S_z = 2\rangle$ occurs. The possible classical or quantum origin of these phenomena is under investigation. Further studies of this and other isostructural materials with differing spin values are in progress. The specific heat studies performed at NHMFL determined the type of (previously unknown) magnetic ordering below 1.8 K in the Cu compound and gave insight into the strength of the zero-field splittings and exchange constants in the Mn and Fe compounds.

¹ Kmety, C.R., *et al.*, Phys. Rev. B, **60**, 60 (1999).

² Kmety, C.R., unpublished results.

Influence of Nearest-Neighbor Coulomb Interactions on the Phase Diagram of the Ferromagnetic Kondo Model

Malvezzi, A., NHMFL

Yunoki, S., NHMFL

Dagotto, E., NHMFL/FSU, Physics

The influence of a nearest-neighbor Coulomb repulsion of strength V on the properties of the Ferromagnetic Kondo model is analyzed using computational techniques.¹ The Hamiltonian studied here is defined on a chain using localized $S=1/2$ spins, and one orbital per site. Special emphasis is given to the influence of the Coulomb repulsion on the regions of phase separation recently discovered in this family of models, as well as on the double-exchange-induced ferromagnetic ground state. When phase separation dominates at $V=0$, the Coulomb interaction breaks the large domains of the two competing phases into small “islands” of one phase embedded into the other. This is in agreement with several experimental results, as discussed in the text. Vestiges of the original phase separation regime are found in the spin structure-factor as incommensurate peaks, even at large values of V . In the ferromagnetic regime close to density $n=0.5$, the Coulomb interaction induces tendencies to charge ordering without altering the fully polarized character of the state. This regime of “charge-ordered ferromagnetism” may be related with experimental observations of a similar phase by Chen, C. H. and Cheong, S.-W., Phys. Rev. Lett., **76**, 4042 (1996). Our results reinforce the recently introduced notion (see e.g., Yunoki, S., *et al.*, Phys. Rev. Lett., **80**, 845 (1998)) that in realistic models for manganites analyzed with unbiased many-body techniques, the ground state properties arise from a competition between ferromagnetism and phase-separation/charge-ordering tendencies.

¹ Malvezzi, A., *et al.*, Phys. Rev. B, **59**, 7033 (1999).

The Electronic Structure of High-Spin Iron(III) Ions in Large Magnetic Clusters

Maniero, A.L., NHMFL

Pardi, L.A., NHMFL and Consorzio INSTM-Italy

Segre, U., Univ. of Modena and Reggio Emilia, Chemistry, and CSSMRE-CNR-Italy

Cornia, A., Univ. of Modena and Reggio Emilia-Italy, Chemistry

Fabretti, A.C., Univ. of Modena and Reggio Emilia-Italy, Chemistry

Gatteschi, D., Univ. of Florence-Italy, Chemistry

Sessoli, R., Univ. of Florence-Italy, Chemistry

The origin of magnetic anisotropy in large magnetic clusters has been the focus of increasing attention since the discovery that high-spin molecules with a large Ising-type anisotropy can behave like single-molecule magnets. The possibility to design and synthesize new magnetic clusters with increased performances, however, requires a deeper understanding of the balance between the different anisotropic contributions (single-ion, dipolar and exchange terms). We have investigated the origin of magnetic anisotropy in a highly symmetric model cluster, namely $[\text{NaFe}_6(\text{OCH}_3)_{12}(\text{pmdbm})_6]\text{ClO}_4$ where $\text{pmdbm} = 1,3\text{-bis}(4\text{-methoxyphenyl})\text{-}1,3\text{-propanedione}$. The compound crystallizes in trigonal space-group $R\bar{3}$ and has a nonmagnetic $S = 0$ ground state. Magnetic anisotropy arises from the presence of thermally-accessible excited magnetic states ($S = 1, 2$, etc.) which show sizeable zero-field splitting (zfs) effects.¹ In particular, the axial zfs of the $S = 1$ state has been precisely determined by high-field torque magnetometry at 0.45 K ($D_1 = 4.3 \text{ cm}^{-1}$).² Dipolar terms (calculated in the point-dipole approximation) account for about 27% of the observed anisotropy only.³ Since exchange-coupled iron(III) compounds should exhibit negligible exchange anisotropies, large single-ion contributions must be present. We attempted to confirm this view through the synthesis and high-frequency EPR of the isostructural compound $[\text{NaGa}_{6-x}\text{Fe}_x(\text{OCH}_3)_{12}(\text{pmdbm})_6]\text{ClO}_4$. The experiment was suggested by the rich EPR spectrum of the iron(III)-doped dimer $[\text{Ga}_{2-x}\text{Fe}_x(\text{OCH}_3)_2(\text{dbm})_4]$ ($\text{Hdbm} = \text{dibenzoylmethane}$; see 1998 NHMFL Annual Report). The EPR spectra of a sample with $x = 0.02$ ca were recorded at frequencies ranging from 109 GHz to 670 GHz using the EMR facility at the NHMFL. A low iron(III) content was used to limit the formation of poly-substituted species. The spectra at 4-40 K show that the $S=5/2$ iron(III) centers have a completely rhombic zfs, with $D_{\text{Fe}} \sim 0.31 \text{ cm}^{-1}$ and $E_{\text{Fe}} \sim 0.10 \text{ cm}^{-1}$. These parameters are to be compared with those found in the $\text{Ga}_{2-x}\text{Fe}_x$ dimer ($D_{\text{Fe}} \sim 0.77 \text{ cm}^{-1}$, $E_{\text{Fe}} = 0.08 \text{ cm}^{-1}$). This result shows that high-spin iron(III) ions in large oxo-clusters may exhibit sizeable magnetic anisotropies. Contrary to what has been suggested previously,¹ however, the magnetic anisotropy of the iron(III) ions in Fe_6 is nonaxial. Since single-ion anisotropies are projected with a negative sign on the S-multiplets, the

positive sign of both D_1 indicates that the easy direction of the single-ion anisotropy tensors is essentially parallel to the cluster axis.⁴

¹ Caneschi, A., *et al.*, Chem.-Eur. J., **2**, 1379 (1996).

² Cornia, A., *et al.*, Phys. Rev. B., **60**, 12177 (1999).

³ Cornia, A., *et al.*, Angew. Chem. Int. Ed. Engl., **38**, 2264 (1999).

⁴ Feola, V., Thesis, University of Modena and Reggio Emilia (1999).

Residual Stress in Thin Films of Strontium-Doped Lanthanum Manganites

Meda, L., NHMFL/FAMU-FSU College of Engineering and MARTECH

Dong, X., NHMFL/FAMU-FSU College of Engineering and MARTECH

Dahmen, K.-H., FSU, Chemistry

Garmestani, H., NHMFL/FAMU-FSU College of Engineering and MARTECH

Interest in the mechanical behavior of thin films in the past few years has increased considerably. It is well known that most deposited thin films are under some kind of residual (internal) stresses that often control their properties.¹

X-ray diffraction (XRD) is a very useful technique for texture analysis and measuring residual strain/stress. Stresses alter the spacing of crystallographic planes in composite (film/substrate) crystals by an amount that usually can be measured by x-ray diffraction.

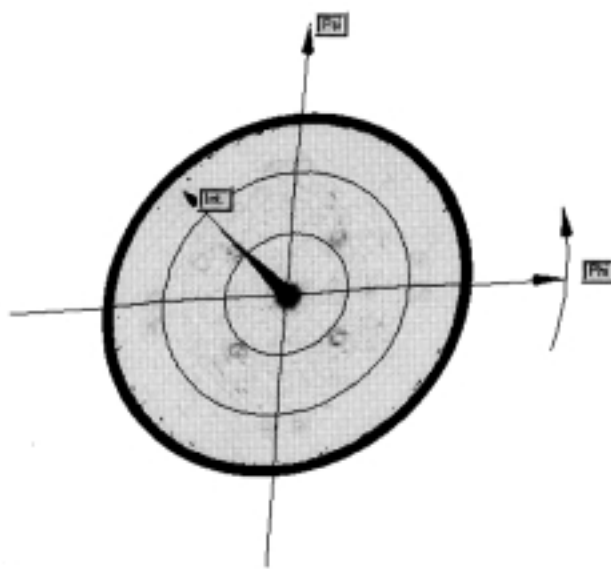


Figure 1. Films deposited on LaAlO_3 exhibit a dominant (001) preferred orientation.

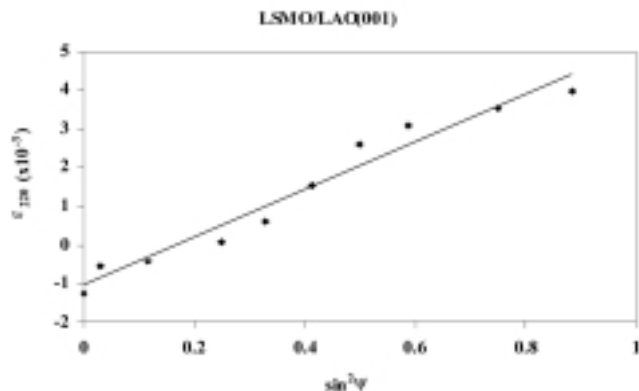


Figure 2. ϵ vs. $\sin^2\psi$ of LSMO on LaAlO_3 (001) using the (220) plane. R = Reuss average, N-Hill = Neerfeld-Hill average, and V = Voigt average.

Films deposited on LaAlO_3 exhibit a dominant (001) preferred orientation (Figure 1) while those on sapphire and Y-ZrO_2 are randomly textured. The macroscopic residual stresses of $\text{La}_{0.67}\text{Sr}_{0.33}\text{MnO}_3$ (LSMO) CVD films are presented following the grain interaction models described by Voigt and Reuss for randomly textured aggregate² assuming a biaxial stress state. Also, the weighted average of the Neerfeld-Hill approach is used. From the plot of the elastic strain (ϵ) vs. $\sin^2\psi$ (Figure 2), the stress can be obtained from the linear regression and the elastic constant are calculated from the compliances of $\text{La}_{0.83}\text{Sr}_{0.17}\text{MnO}_{3.3}$

$$\epsilon_{\psi}^{\text{hkl}} = \frac{d_{\psi}^{\text{hkl}} - d_0^{\text{hkl}}}{d_0^{\text{hkl}}} = \left[\frac{1+\nu}{E} \sin^2(\psi) - 2\frac{\nu}{E} \right] \sigma_{//} \quad (1)$$

In plane residual stress ranging from 412 to 976 MPa (Figure 2) was calculated for LSMO films deposited on Y-ZrO_2 , Sapphire, and LaAlO_3 . The results are summarized in Table 1.

Table 1. Lattice mismatch, % strain, and stress of as-deposited LSMO films.

| Film/Substrate | Lattice Mismatch | % Strain | | Stress (MPa) | | |
|------------------------------|------------------|----------|------|--------------|-----|--------|
| | | // | ⊥ | R | V | N-Hill |
| LSMO/ LaAlO_3 (001) | 2.558 % | 0.65 | 0.05 | 425 | 665 | 518 |
| LSMO/ Y-ZrO_2 (001) | 6.725 | 0.03 | 0.66 | 453 | 552 | 708 |
| LSMO/Sapphire(0001) | 26.739 | 0.21 | 0.72 | 624 | 761 | 976 |

*R = Reuss V = Voigt N-Hill = Neerfeld-Hill

¹ Hoffman, R.W., Physics of thin films, **3**, 211 (1996).

² Noyan, I.C. and Cohan, J.B., *Residual Stress*, Springer-Verlag, NY 1987.

³ Thompson, J.D., *et al.*, Phys. Rev. B, **57**, 5094 (1998).

Breaking of Atomic Symmetry at High Magnetic Field Strengths

Meersmann, T., Univ. of California at Berkeley, Chemistry
Pavlovskaya, G., Univ. of California at Berkeley, Chemical Engineering

It is usually assumed that the strong magnetic fields used in NMR spectroscopy will not affect the molecular or atomic structure of our samples. However, in the light of the previous discoveries at the NHMFL¹ and subsequent theoretical work at Berkeley,² there is some reason to believe that this assumption is wrong. Unfortunately, the effect is very subtle and difficult to study at the field strengths currently available for NMR spectroscopy. Earlier attempts to observe this effect had failed³ and so far it can only be detected by one of the most sensitive detectors available for this purpose: Xenon-131 gas-phase NMR spectroscopy.

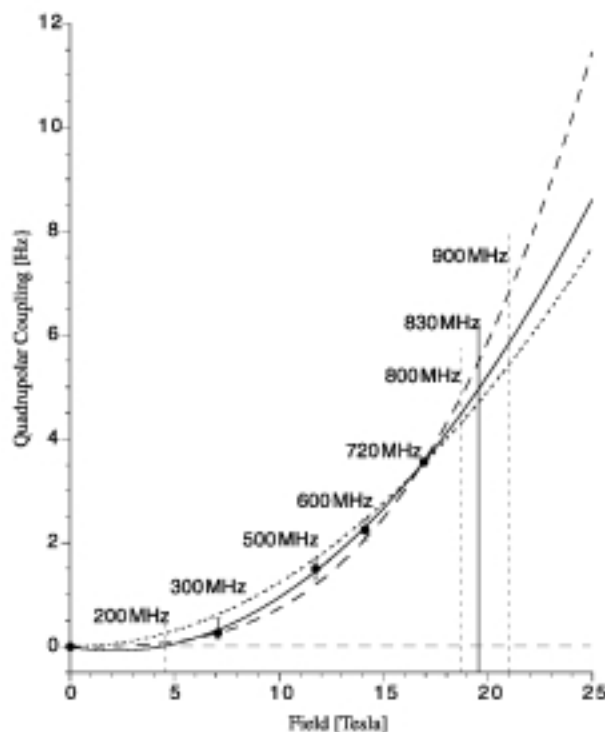


Figure 1. Quadrupolar splitting observed in gas phase xenon-131 NMR (filled circles) as a function of the applied magnet field strength (units in proton frequency). The solid line represents a best fit of function with linear and quadratic field dependence (dashed lines: best fit of quadratic or cubic dependence).

This method is very sensitive due to the large electron cloud of the xenon atom that is easily distorted thus resulting in an electric field gradient (EFG) at the location of the nucleus. The nucleus of the isotope xenon-131 (spin $S=3/2$) possesses a large electric quadrupole moment which will interact with the EFG. The resulting quadrupolar coupling serves as a sensitive detector for the presence of an EFG and therefore for a distortion of the electron cloud. In the pure gas phase, the xenon atom assumes spherical symmetry and no coupling should occur in gaseous xenon-131 if interactions of xenon atoms with the surrounding container walls are excluded. The discovery of

a surface independent quadrupolar splitting indicates that an electrical polarization of the xenon electron cloud is induced by the magnetic field. Closer inspection shows a linear and quadratic dependence of the quadrupolar coupling upon the applied magnetic field (see Figure 1). Salsbury and Harris² estimated the size of the effect to be in agreement with observed splitting. They also expected the presence of a linear term in addition to the quadratic term in particular for elements with very high atomic numbers Z such as xenon.

We studied the effect of a 10 kV DC electric field applied on xenon-131 at 16.92 T (720 MHz proton frequency), however there was no appreciable change observable in the quadrupolar splitting. In order to explore the magnetic field effect further we investigated the influence of high magnetic fields on ^{83}Kr ($S=9/2$) at 16.92 T. No observable splitting within the 1.2 Hz linewidth was generated by the magnetic field. This should change once stronger magnetic fields with sufficient homogeneity become available and may also lead to related discoveries in other systems. Higher fields for NMR spectroscopy should provide us with important insights about the precise laws that rule the field induced distortions of the electron shell.

¹ Meersmann, T., Phys. Rev. Lett., **81**, 1211 (1998).

² Salsbury, J.F.R., J. Chem. Phys., **109**, 8338 (1998).

³ Filsinger, B., J. Mag. Res., **125**, 280 (1997).

Magnetic Phase Transitions in UNiAl and UNiGe Under High Magnetic Field and Pressure

Mikulina, O., Czech Academy of Science

Kamarád, J., Czech Academy of Science

Lacerda, A., NHMFL/LANL

Sechovsky, V., Charles Univ., Prague, Metal Physics

Nakotte, H., New Mexico State Univ. at Las Cruces,
Physics

Beyermann, W., Univ. of California at Riverside, Physics

The main motivation was to study magnetic phase transitions in antiferromagnets UNiAl and UNiGe¹ under combination of a magnetic field and a hydrostatic pressure. Since the magnetic phase transitions in UNiAl and UNiGe are accompanied by electrical resistivity (ρ) anomalies, magnetism in these materials can be studied to certain extent by a relatively simple measurement of ρ as a function of temperature and magnetic field, $\rho(T,B)$, at selected hydrostatic pressures.

Single crystals of UNiAl and UNiGe grown by a modified Czochralski tri-arc method were used. The magnetic field B was applied along the c -axis and the electrical current I was parallel ($I \parallel c$) and in case of UNiAl also perpendicular to this direction ($I \perp c$). The ρ was measured by an AC Resistance Bridge (model LR-700, Linear Research INC) using a standard four probe method. The pressure up to 1 GPa was generated

using a Cu-Be piston-cylinder device with a mixture of mineral oils as a pressure transmitting medium. The temperature was measured using a calibrated Cernox thin film resistance sensor that was mounted on an outer surface of the pressure cell. At selected hydrostatic pressures, we measured the temperature dependence of the electrical resistivity of UNiAl at fixed fields and the field dependence of the resistivity at fixed temperatures. All the measurements were performed at the NHMFL at Los Alamos using the 20 T superconducting magnet. In all cases magnetic field up to 18 T was applied along the c -axis.

UNiAl: Application of pressure leads to a gradual suppression of values of the Néel temperature T_N (at -1.5 K/GPa) and the critical field B_c of the metamagnetic transition (this behavior can be approximated by $B_c(P) = B_c(0) + a_P P^n$, where $B_c(0) = 11.33 \pm 0.02 \text{ T}$ is the critical field at ambient pressure and parameters $n = 2.48 \pm 0.10$ and $a_P = -0.62 \pm 0.02 \text{ T/GPa}^2$ yield in an estimate of the critical pressure for magnetism in UNiAl around 3 GPa). A sudden change of the low-temperature part of the $\rho(T)$ curve for $i \perp c$ upon application of pressure indicates a new pressure-induced scattering mechanism presumably connected with magnetic phenomena. These phenomena can be attributed to the itinerant nature of 5f magnetic moments.

UNiGe: The $\rho(T)$ curves measured at several pressures indicate that T_N in UNiGe is nearly unaffected by pressure up to 1 GPa. There are two metamagnetic transitions in this material. The respective critical fields B_1 and B_2 are considerably enhanced with pressure although the relative ρ_c steps at the MT's and the hysteresis remain nearly unchanged. Assuming linear pressure effects, our data lead to $B_1/p = 2.4 \text{ T/GPa}$, $B_2/p = 3.3 \text{ T/GPa}$ and $\ln B_1/p = 0.47 \text{ GPa}^{-1}$, $\ln B_2/p = 0.32 \text{ GPa}^{-1}$, respectively. The pressure-induced enhancement of B_1 and B_2 clearly implies that the antiferromagnetic exchange interactions in UNiGe increase with reducing interatomic distances. This fact in conjunction with the pressure independence of the critical temperatures corroborate the present understanding of UNiGe as a material whose 5f-electrons are more localized than ones of the other members in the series such as UNiAl.

Acknowledgements: This work was performed under the auspices of the NSF-Division of International Programs.

¹ Sechovsky, V. and L. Havela, L., in: *Handbook of Magnetic Materials*, Vol. 11, K.H.J. Buschow, eds. (Elsevier Science B.V., Amsterdam, 1998) p. 1.

Phase Separation Scenario for Manganese Oxides and Related Materials

Moreo, A., NHMFL/FSU, Physics

Dagotto, E., NHMFL/FSU, Physics

Yunoki, S., NHMFL

Recent computational studies of models for manganese oxides have revealed a rich phase diagram, which was not anticipated in early calculations in this context performed in the 1950s

and 1960s.¹ In particular, the transition between the antiferromagnetic insulator state of the hole-undoped limit and the ferromagnetic metal at finite hole density was found to occur through a mixed-phase process. When extended Coulomb interactions are included, a microscopically charged inhomogeneous state should be stabilized. These phase separation tendencies, also present at low electronic densities, influence the properties of the ferromagnetic region by increasing charge fluctuations. Experimental data reviewed here by applying several techniques for manganites and other materials are consistent with this scenario. Similarities with results previously discussed in the context of cuprates are clear from this analysis, although the phase segregation tendencies in manganites appear stronger.

¹ Moreo, A., *et al.*, Science, **283**, 2034 (1999).

Pseudogap Formation in Models for Manganites

Moreo, A., NHMFL/FSU, Physics

Dagotto, E., NHMFL/FSU, Physics

Yunoki, S., NHMFL

The density-of-states (DOS) and one-particle spectral function $A(k, \omega)$ of the one- and two-orbital models for manganites, the latter with Jahn-Teller phonons, are evaluated using Monte Carlo techniques.¹ Unexpectedly robust pseudogap (PG) features were found at low- and intermediate-temperatures, particularly at or near regimes where phase-separation occurs as $T=0$. The PG follows the chemical potential and it is caused by the formation of ferromagnetic metallic clusters in an insulating background. It is argued that PG formation should be generic of mixed-phase regimes. The results are in good agreement with recent photoemission experiments for $\text{La}_{1.2}\text{Sr}_{1.8}\text{Mn}_2\text{O}_7$.

¹ Moreo, A., *et al.*, Phys. Rev. Lett., **83**, 2773 (1999).

Spectroscopic Studies of α' - NaV_2O_5 at 60 T

Musfeldt, J.L., State Univ. of New York at Binghamton

Kim, Y.M., NHMFL

Crooker, S., NHMFL

After the discovery of a low-temperature spin-gapped phase in α' - NaV_2O_5 , this compound rapidly attracted attention as the second inorganic spin-Peierls material.¹ More recently, structural studies have called into question the assumed nature of the spin chains, pairing mechanism, and dimerization, and the character of the low-temperature phase is now controversial.²

In order to probe the rich electronic structure of α' - NaV_2O_5 , we have extended previous optical measurements³ to very high magnetic fields using the 60 T “long-pulse” magnet in order to search for changes in electronic structure that might indicate a dimerized \rightarrow incommensurate phase boundary in α' - NaV_2O_5 . Observation of such a boundary and a spin-Peierls-like phase diagram will support the spin-Peierls picture, whereas absence of such a phase boundary will give credence to the spin-gap explanation.

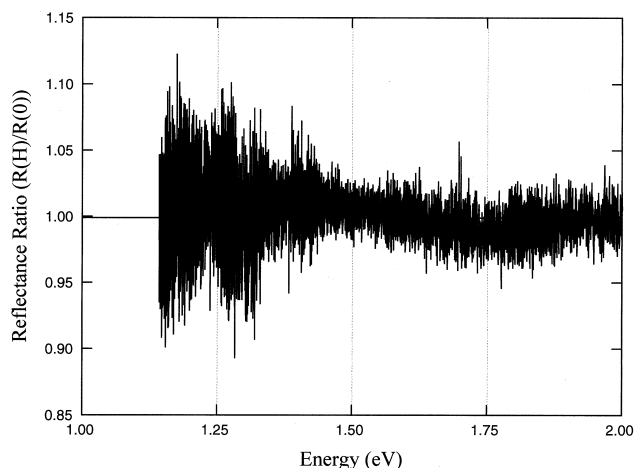


Figure 1. Unpolarized reflectance ratio data of α' - NaV_2O_5 at 2 K.

Preliminary unpolarized reflectance ratio (R) data has been collected on α' - NaV_2O_5 at 2 K (Figure 1). Here, $R = R(60 \text{ T})/R(H = 0 \text{ T})$; the reflectance ratio is essentially a normalized response that highlights reflectance changes with applied field. Small deviations from unity are observed below 2 eV. The broad bands are in line with previous optical probes of R in α' - NaV_2O_5 .³ Coexistence of both spin-Peierls and charge ordering interactions is also a possibility.

Future work will focus on several issues. Experimentally, we need to improve the probe by adding a vacuum jacket and a heater coil to warm the sample between shots (to avoid sample fatigue); also, we will use Polaroid films to collect the polarized R of α' - NaV_2O_5 , which is expected to display larger changes with applied field. Finally, we hope to be able to use the “flat top” character of the magnet pulse to do more averaging of the signal at 60 T. Once reliable data has been collected, the R will be analyzed in terms of the absolute optical spectra and electronic structure calculations.

¹ Isobe, M. and Ueda, Y., J. Phys. Soc. Jpn., **65**, 1178 (1996).

² Musfeldt, J.L., *Spin Peierls Materials*, in Magnetism: From Molecules to Materials, edited by J.S. Miller and M. Drillon, submitted.

³ Long, V.C., *et al.*, Phys. Rev. B, **60**, 15721 (1999).

Spectroscopic Studies of α' - NaV_2O_5 in High Magnetic Fields

Musfeldt, J.L., State Univ. of New York at Binghamton, Chemistry

Wei, X., NHMFL

Long, V.C., SUNY-Binghamton, Chemistry

Zhu, Z., SUNY-Binghamton, Chemistry

Whangbo, M., North Carolina State Univ., Chemistry

After the discovery of a low-temperature spin-gapped phase in α' - NaV_2O_5 , this compound rapidly attracted attention as the second inorganic spin-Peierls material.¹ More recently, structural studies have called into question the assumed nature of the spin chains, pairing mechanism, and dimerization, and the character of the low-temperature phase is now controversial.² In order to probe the rich electronic structure of α' - NaV_2O_5 , we have extended previous optical measurements to higher energies, and to the low-temperature and high magnetic field regimes.³ Our goal is to characterize the competing broken symmetry ground states in α' - NaV_2O_5 .

The polarized electronic excitations in the frequency dependent conductivity of α' - NaV_2O_5 are interpreted according to our extended Huckel tight binding polarized band structure

calculations.³ Strong bands near 1 eV in both chain and rung directions are attributed to V d \rightarrow d (on-rung) transitions. O p \rightarrow V d charge transfer excitations appear at higher energy. We estimate the optical gap to be ≈ 3.3 (3.5) eV in the rung (chain) direction. Greater oscillator strength in the rung (compared to the chain polarization) is consistent with d-block bands that are less dispersive along the rung direction.

Reflectance ratios, measured along both the chain and rung directions of α' - NaV_2O_5 , reveal broad polarization-dependent changes through the 36 K phase transition (Figure 1).³ In the past, we have successfully used changes in the optical response to map out the boundaries of the H – T phase diagram in CuGeO_3 . Although the electronic structure changes of α' - NaV_2O_5 are quite different than those of CuGeO_3 , the use of optical spectroscopy for following the phase transitions is still applicable. Thus, we made both zero and high-field (H = 28 T) measurements of the reflectance ratio in α' - NaV_2O_5 to determine the field dependence of T_c . We find a 3 K reduction in T_c at 28 T, consistent with a possible quadratic field dependence of T_c .

¹ Isobe, M. and Ueda, Y., J. Phys. Soc. Jpn., **65**, 1178 (1996).

² Musfeldt, J.L., "Spin Peierls Materials," in Magnetoscience: From Molecules to Materials, edited by J.S. Miller and M. Drillon, submitted.

³ Long, V.C., *et al.*, Phys. Rev. B, **60**, 15721 (1999).

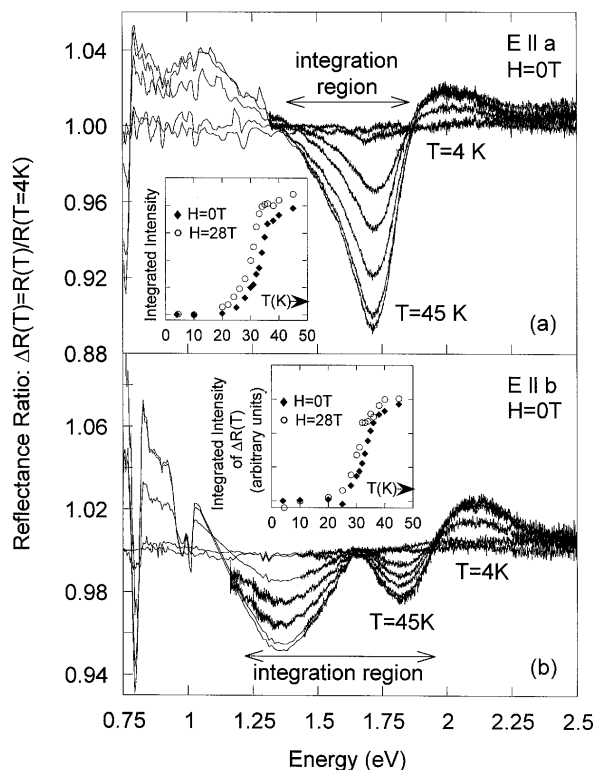


Figure 1. Temperature dependence of the zero-field reflectance ratios for the (a) E // a and (b) E // b polarizations. The inset for each polarization shows the integrated intensities of the reflectance ratio features vs. temperature. Empty circles: zero-field data; solid diamonds: 28 T data (not shown).

High Frequency EPR Spectroscopy of Neutral and One-Electron Reduced Dodecanuclear Manganese Complexes

Nakano, M., Univ. of California at San Diego, Chemistry

Yoo, J., UCSD, Chemistry

Krzystek, J., NHMFL

Maniero, A.L., NHMFL

Christou, G., Indiana Univ., Chemistry

Hendrickson, D.N., UCSD, Chemistry

Dodecanuclear manganese complexes of the type $(\text{Mn}_{12}\text{O}_{12}(\text{O}_2\text{CR})_{16}(\text{H}_2\text{O})_4)$ where R is an organic substituent have been termed as single-molecule magnets (SMM).¹ SMMs function as single isolated magnets and the properties are of molecular origin and not from a bulk property. Below a critical temperature, these molecules are capable of becoming magnetized and exhibit slow magnetization relaxation due to an appreciable energy barrier for the reversal of the direction of its magnetization. The energy barrier results from a combination of a large ground spin state and negative magnetic anisotropy. The mechanism of the relaxation process has been an actively pursued research topic. The relaxation in SMMs occurs via a thermally activated process or via quantum mechanical tunneling. In the former mechanism, the relaxation occurs by climbing up and over the energy barrier via a phonon mediated Orbach process whereas in the latter mechanism the relaxation occurs via tunneling through the barrier.² Exactly which factors

play the largest role in the tunneling process are yet to be determined.

High frequency EPR can provide some qualitative understanding of the tunneling process.³ It is believed that the higher order crystal field effects in the spin Hamiltonian, in particular the fourth order terms are responsible for the tunneling process. Through the careful analysis of the parallel and perpendicular components in the EPR spectrum, these higher order terms can be determined. A series of neutral and one electron reduced dodecanuclear manganese complexes were studied by high frequency EPR spectroscopy.

¹ Friedman, J.R., *et al.*, Phys. Rev. Lett., **76**, 3830 (1996).

² Villain, J., *et al.*, Europhysics Lett., **27**, 159 (1994).

³ Barra, A.-L., Phys. Rev. B, **56**, 8192 (1998).

Finite Size Effects on Spin Glass Dynamics

Orbach, R.L., Univ. of California at Riverside,
Chancellor's Office

Wood, G.G., UC, Riverside

Hamann, J., CEA, Saclay, France

Vincent, E., CEA, Saclay, France

Joh, Y.G., NHMFL/LANL

Boebinger, G.S., NHMFL/LANL

The recent identification of a time and temperature dependent spin glass correlation length¹, $\zeta(t, t_w)$, has consequences for samples of finite size. Qualitative arguments are given on this basis for departures from t, t_w scaling for the time decay of the thermoremanent magnetization, $MTRM(t, t_w, T)$, where t is the measurement time after a "waiting time" t_w , and for the imaginary part of the ac susceptibility, $\chi''(\omega, t)$. Consistency is obtained for a more rapid decay of $MTRM(t, t_w, T)$ with increasing t_w when plotted as a function of t_w , for the deviation of the characteristic time for $MTRM(t, t_w, T)$ from a linear dependence upon H^2 at larger values of H , and for the deviation of the decay of $\chi''(\omega, t)$ from ωt scaling² upon a change in magnetic field at large values of ωt . Departures from scaling arise when the spin glass correlation length becomes of the order of or smaller than the particle size associated with the existence of small crystallites or particles in the spin glass sample.

Future experiments and numerical simulations, leading to the extraction of the particle size distribution, $P(r)$, are planned with specific attention to what can be learned from experimental protocols. SEM measurements of the particle size distribution will lead to explicit experimental consequences, setting the stage for a consistency check on the entire model.^{1,3} It is remarkable that the behavior of magnetization measurements in the time domain could so directly depend upon the physical size parameters of the sample particulates.

¹ Joh, Y.G., *et al.*, Phys. Rev. Lett., **82**, 438 (1999).

² Vincent, E., *et al.*, Phys. Rev. B, **52**, 1050 (1995).

³ Joh, Y.G., *et al.*, Phys. Rev. Lett., **77**, 4648 (1996).

High Field EPR Signal for Short Chains in Non-Magnetically Doped Y_2BaNiO_5

Saylor, C.A., NHMFL

Van Tol, H., NHMFL

Cheong, S.-W., Rutgers Univ., Physics

Brunel, L.-C., NHMFL

Y_2BaNiO_5 ¹ is an ideal Haldane Gap^{2,3} material. In addition to its large Haldane Gap and its relatively small anisotropy in comparison with NENP, it is an excellent material for studying finite chain length effects because its crystals are grown by solid state reaction. This process permits better control of the non-magnetic doping concentration as well as greater non-magnetic doping concentrations.

An interesting feature of Haldane Gap materials is that the ground state for a semi-infinite finite length chain ($L > 40$) is four-fold degenerate.⁴ This four-fold degeneracy can be described by two many-body $S=1/2$ spins⁵ at the ends of the chain. In short chains, this four-fold degeneracy is split. This splitting can be described by the interaction of the two many-body $S=1/2$ chain end spins, which splits the four-fold degenerate state into an $S=0$ and an $S=1$ state. The $S=1$ state is further split by the anisotropy in the exchange and the single ion anisotropy for the $S=1$ sites that make up the chain.

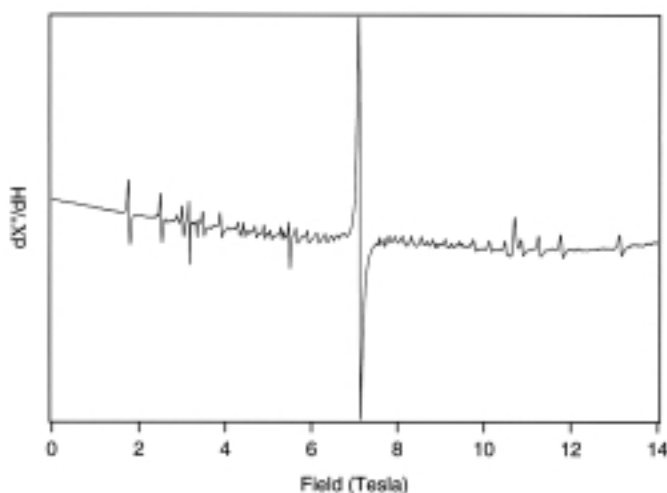


Figure 1. High frequency EPR spectrum (218 GHz) of Y_2BaNiO_5 doped with 2% Mg. The low and high field lines are the result of the short chain lengths in which the two intrachain $S = 1/2$ spins are effectively coupled to produce an $S = 1$ state. (Temperature: 5 K)

The strength and sign of the exchange interaction between the many-body $S=1/2$ spins is strongly dependent on the chain length. Figure 1 shows the EPR signal at 218 GHz for $T = 5$ K and the field parallel to the C-axis. At approximately 7.2 T we see the EPR signal for the many-body $S=1/2$ spins for the semi-infinite chain lengths. The EPR signals on either side of 7.2 T are at first minimal and then increase in both directions as the lengths of the finite chains become shorter and the splitting of the $S=1$ state increases.

In conclusion, the EPR spectrum confirms a Haldane system for short chains has four closely spaced energy levels separated from the continuum of excited states by the Haldane Gap with the distribution of chain lengths defined by an exponential distribution resulting in the decrease in signal intensity with increasing chain length. The next step of this experiment is to accurately map the angular dependence of the resonant fields for the different length chains in order to determine the anisotropy of exchange and the single ion anisotropy for the Ni site.

- ¹ Xu, G.Y., *et al.*, Phys. Rev. B, **54**, 6827 (1996).
- ² Haldane, F.D.M., Phys. Rev. Lett., **50**, 1153 (1983).
- ³ Haldane, F.D.M., Phys. Lett. A, **93**, 464 (1983).
- ⁴ Kennedy, T., J. Phys. Condensed Mat., **2**, 5737 (1990).
- ⁵ Affleck, I., *et al.*, Phys. Rev. Lett., **59**, 799 (1987).

High Field EPR Measurements on Tm^{3+} Ions

Tagirov, M.S., Kazan State Univ., Russia, Physics
 Tayurskii, D.A., Kazan State Univ., Russia, Physics
 Van Tol, J., NHMFL
 Brunel, L.-C., NHMFL

The lanthanide series of tripositive rare-earth ions has been extensively studied in the past at conventional EPR frequencies, however some of the ions with an even number of f-electrons have totally escaped EPR detection due to the large zero-field-splitting in these ions. One of these EPR-silent ions is Tm^{3+} (a $4f^{12}$ system with a $J=6$ groundstate). Recently, however, we have investigated the EPR spectra Tm^{3+} ions at moderately high magnetic fields (up to 11.5 T) in lanthanumethylsulphate and thuliumethylsulphate single crystals (Phys. Rev. Lett., **77** (1996), 3459) at very high frequencies in the range of 1-1.6 THz. This study left us with several questions. The linewidth of the transition varies considerably as a function of the field, and the reasons for this are not understood. We would like to measure these linewidths over a larger field range and measure also a second high-field transition. Furthermore in the pure thulium-ethylsulphate we could observe a considerable mixing of the higher spin states with vibrational levels of the lower spin state causing the EPR line to split. In order to answer these questions we have currently started a study of a similar system, Tm^{3+} in LaCl_3 (0.5%). The crystal field is very similar to the one of ethylsulphate, but spin-spin effects and vibrational energies are different, and should help us to understand better the interaction with the vibronic states. In order to get appreciable energy changes of the sublevels of the J-multiplet the Zeeman field should be of the order of the zero-field splittings and thus in the range of 10 to 60 T.

We have performed initial measurements in the 25 T Keck magnet, at frequencies in the range of 525 up to 1800 GHz. A typical EPR spectrum is shown in Figure 1. The sharp features are Nd^{3+} and Gd^{3+} impurities ($h\nu \gg kT$ so only the $\text{Gd } -7/2$ to $-5/2$ transition is observed) and the much broader transitions at 17.4 and 21.2 T are assigned to the Tm^{3+} ions. These results

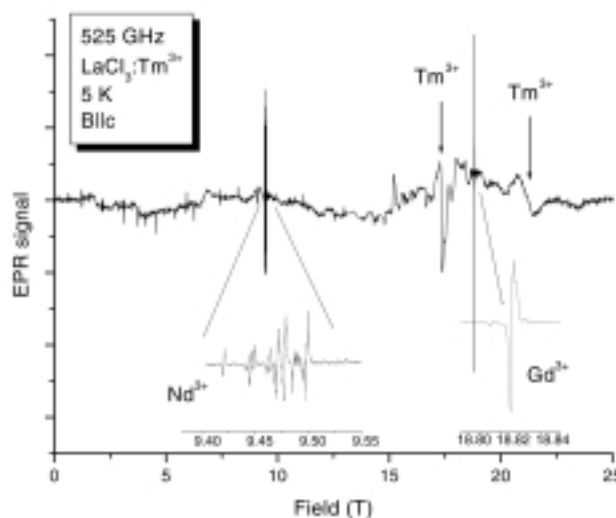


Figure 1. EPR spectrum of Nd^{3+} and Gd^{3+} impurities in Tm^{3+} doped LaCl_3 .

allowed us to determine that the crystal field splitting from the ground singlet to the first excited doublet to be $21(1) \text{ cm}^{-1}$, but so far the limited number of measured frequencies and crystal orientations do not allow a reliable linewidth analysis.

Magnetic Properties of Small Iron Clusters in Sodalite

Trill, H., Univ. of California at Santa Barbara, Chemistry
 Srdanov, V.I., Univ. of California at Santa Barbara, Chemistry
 Kim, Y., NHMFL
 Lacerda, A., NHMFL/LANL

The NSF supported research at UCSB led recently to the discovery of soft ferromagnetism in sodalites containing small Fe clusters. When synthesized from kaoline, halogen-sodalites incorporate about 1% of Fe^{3+} impurities. The exposure of such a sodalite to sodium vapor reduces Fe^{3+} to Fe^0 , which are deemed mobile at elevated temperatures. The random walk of Fe^0 atoms leads to their coalescence into small $(\text{Fe}^0)_x$ clusters embedded inside sodalite cages whose free volume is on the order of 300 \AA^3 . Larger iron clusters can also form by breaking a few Si-O and Al-O bonds between two sodalite cages. Besides $(\text{Fe}^0)_x$ clusters of various sizes, our samples also contain a certain number of “free” Fe^0 atoms. In addition, sodalite cages unoccupied by the halogen anion can host a $\{4\text{Na}^+(\text{e}^-)\}$ type of F centers which couple magnetically below 50 K.¹

The system described above, consisting of small magnetic clusters embedded in the spin glass matrix, is known as “mictomagnet” or “cluster glass”.² Like in true spin glasses, magnetically coupled spins in a cluster glass system are expected to freeze below certain temperatures, but should also show enhanced remnance and peculiar hysteretic behavior. Ferromagnetically coupled cluster glass should display both

large magnetization and susceptibility. Indeed, the iron clusters in sodalite exhibit blocking temperatures of up to 150 K, susceptibilities on the order of 0.5 emu/g and hysteresis curves with tunable widths (see Figure 1).³ The control of the coercive field magnitude, H_c , is accomplished in the synthesis by varying the percentage of cages occupied by halogen anion. Such cages slow down the diffusion of Fe^0 atoms yielding smaller $(\text{Fe}^0)_x$ clusters.

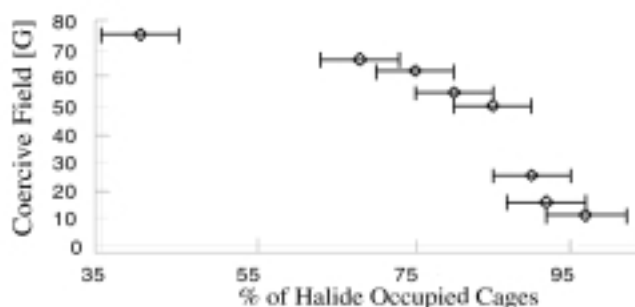


Figure 1. Iron clusters in Br-sodalites.

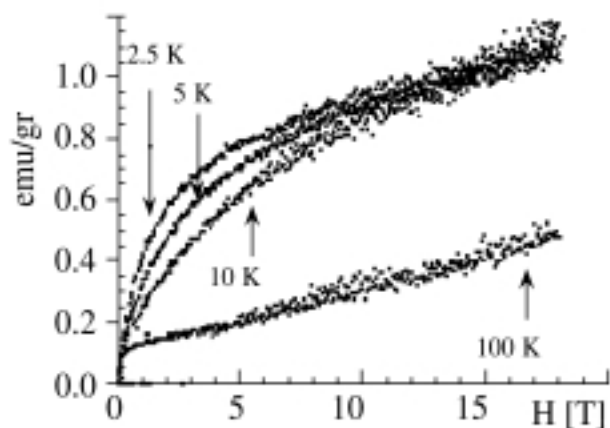


Figure 2. Saturation magnetization measurements.

The saturation magnetization measurements in Figure 2 reveal three distinct contributions to the overall susceptibility. The relatively small magnetization due to “free” Fe^0 atoms, clearly visible in the 100 K run, saturates at low fields. The susceptibility due to ferromagnetically coupled $(\text{Fe}^0)_x$ clusters, prevails below blocking temperature but requires 5 T at 2.5 K to saturate. Finally, the susceptibility contribution due to iron species coupled by a long-range exchange interaction does not saturate even at 18 T. It is uncertain to what extent, if at all, the $\{4\text{Na}^+(\text{e}^-)\}$ centers mediate exchange coupling between the iron species.

¹ Srdanov, V.I., *et al.*, Phys. Rev. Lett., **80**, 2449 (1998).

² Mydosh, J.A., Spin Glasses, Taylor & Francis, London, 1993.

³ Trill, H., Diploma Thesis, University of Munster, 1999.

Studies of Novel Low Dimensional Magnets

Watson, B.C., UF, Physics

Meisel, M.W., UF, Physics

Jensen, D.A., UF, Chemistry

Fanucci, G.E., UF, Chemistry

Talham, D.R., UF, Chemistry

Hall, D., NHMFL

A rich variety of novel phenomena is being explored in low dimensional magnets. While our work with one and two dimensional magnets is continuing, we have expanded into the area bridging these two regimes, namely into the study of magnetic spin ladders. The significance of understanding the properties of magnetic spin ladders has been reviewed by Dagotto and Rice.¹ Experimentally, macroscopic properties alone are usually insufficient to distinguish a spin ladder from another possible description such as an alternating chain.²

Our work involves the study of two spin $S = 1/2$ materials, which we refer to as BPCB, $[(\text{pipdH})_2\text{CuBr}_4]$,³ and MCCL, $(\text{CH}_3)_2\text{NH}_2\text{CuCl}_3$.⁴ The magnetic structures of BPCB and MCCL consist of weakly interacting dimer units that are arranged in ladder-like or alternating chain structures, respectively. Using single crystal and powder samples, the magnetizations of these systems have been measured from 1.8 K to 300 K in fields up to 5 T using a commercial SQUID magnetometer. These measurements were extended up to 25 T using a vibrating sample magnetometer (VSM). Employing standard models, the data have been fit to determine the magnetic exchange energies, namely J_\perp 13 K and J_\parallel 2 K for BPCB and J_1 2.8 K and J_2 1.2 K for MCCL. In order to determine the appropriate magnetic ground states and their dynamical properties, these investigations are being combined with microscopic studies of NMR and neutron scattering using deuterated specimens.

¹ Dagotto, E. and Rice, T. M., Science, **271**, 618 (1996).

² Garrett, A.W., *et al.*, Phys. Rev. Lett., **79**, 745 (1997).

³ Patyal, B.R., *et al.*, Phys. Rev. B, **41**, 1657 (1990).

⁴ Willett, R.D., J. Chem. Phys., **44**, 39 (1966).

High Field Magnetotransport in Half-Metallic Chromium Dioxide

Watts, S.M., FSU, Center for Materials Research and Technology (MARTECH)

Wirth, S., FSU, MARTECH

von Molnár, S., FSU, MARTECH

Barry, A., Trinity College, Dublin, Ireland, Physics

Coey, J.M.D., Trinity College, Dublin, Ireland, Physics

Chromium dioxide has long been an important material in the magnetic recording industry. The only binary oxide to be a

metallic ferromagnet, there has been a renewed interest in the material in recent years because it has been predicted to be a half-metal,¹ for which the conduction electrons are completely spin-polarized. Thin films of CrO₂ might therefore be useful in spin-electronics. We have been studying basic magnetotransport properties of films fabricated in Dublin via the high-pressure, thermal decomposition of CrO₃.

The Hall effect is especially interesting, showing a sign reversal from positive to negative with increasing magnetic field. The sign reversal is shifted rapidly to higher fields as the temperature is increased. The data are well described with a simple two-band model, which indicates the presence of highly mobile holes ($\mu_h = 0.25 \text{ m}^2/\text{Vs}$) along with a factor 400 larger number (0.4 per Cr atom) of less mobile electrons. Figure 1 shows high field Hall effect measurements for temperatures between 10 and 100 K made at the NHMFL superconducting magnet facilities in order to track the two-band parameters as a function

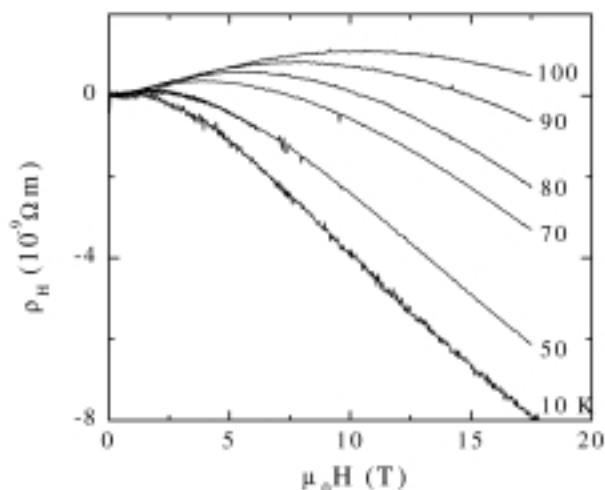


Figure 1. Hall effect for CrO₂ on (110) TiO₂, Dublin sample. Low field curvature in 100 K data is due to the contribution of the anomalous Hall effect.

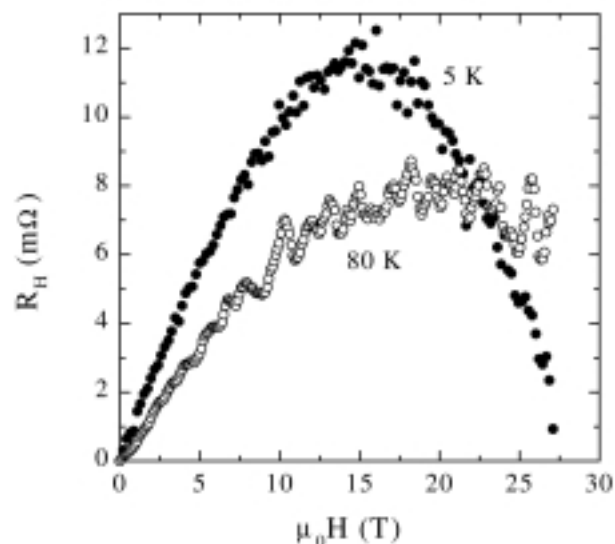


Figure 2. Hall effect for CrO₂ on (100) TiO₂, CVD sample.

of temperature. Our data² has led us to conclude that both holes and electrons experience an onset of single-magnon scattering as the temperature is raised through 80 K—a thermal energy much less than the predicted energy gap of $\sim 1 \text{ eV}$ between majority and minority spin states that should prohibit spin-flip scattering processes.

The small number of highly mobile holes at low temperatures suggests that de-Haas Shubnikov oscillations might be observable in the MR. We were not able, however, to detect such oscillations at 30 mK and magnetic fields of 18 T obtained in SCM-1 with the dilution refrigerator at the NHMFL. Transport methods to detect quantum oscillations may not be appropriate when there are both large and small Fermi surfaces present.

During this study, magnetotransport data for a CrO₂ film produced by an atmospheric pressure, chemical vapor deposition (CVD) technique were published³ that showed a positive linear Hall effect up to 4 T. We obtained a sample from this group in order to see if the high field behavior would be consistent with our results. Figure 2 shows low temperature Hall effect measurements at magnetic fields up to 27 T at the NHMFL that demonstrate that there is indeed a high field sign-reversal in the CVD film. We do not fully understand the differences in magnetotransport between the two types of CrO₂ films, but the basic conclusions from the work on the Dublin films² are consistent with the CVD film results.

- ¹ Schwartz, K., *J. Phys. F*, **16**, L211 (1986). More recently, see Korotin, M.A., *et al.*, *Phys. Rev. Lett.*, **80**, 4305 (1998); Mazin, I.I., *et al.*, *Phys. Rev. B*, **59**, 411 (1999).
- ² Watts, S.M., *et al.*, (to be published, *Phys. Rev. B*).
- ³ Li, X.W., *et al.*, *J. Appl. Phys.*, **85**, 5585 (1999).

High Frequency EPR Spectroscopy of Polynuclear Transition Metal Complexes

Yoo, J., Univ. of California at San Diego, Chemistry
 Nakano, M., UCSD, Chemistry
 Krzystek, J., NHMFL
 Maniero, A.L., NHMFL
 Christou, G., Indiana Univ., Chemistry
 Hendrickson, D.N., UCSD, Chemistry

Interest in polynuclear complexes have been growing in recent years due to the fact that these molecules generally possess large spins¹ thus making them attractive as potential nanoscale magnetic materials and the ultimate high-density storage device. Molecules of this type are known to retain magnetic moments below the so-called blocking temperature (T_B) and have been termed single-molecule magnets (SMMs).² Two requirements are necessary for SMMs, a large spin in the ground state and a Ising type magnetic anisotropy. Both give rise to an activation barrier for the reversal of the direction of magnetization. SMMs are characterized by a frequency dependent out-of-phase (χ_M'') AC susceptibility response and steps on magnetization hysteresis loops which have been attributed to quantum tunneling of

magnetization.³ To date, only a few molecules are known to function as SMMs and ongoing studies have focused on finding new examples of SMMs to better understand the mechanism of quantum tunneling phenomenon as well as trying to increase T_B .

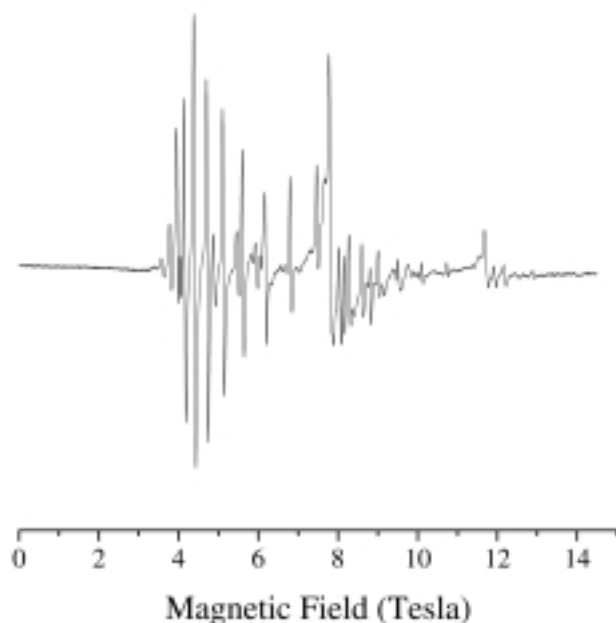


Figure 1. 218 GHz HF-EPR spectrum of polycrystalline $(\text{Mn}_4(\text{O}_2\text{CMe})_2(\text{pdmH})_6)(\text{ClO}_4)_2 \cdot 2.5\text{H}_2\text{O}$ oriented in magnetic field at 30 K.

The main motivation behind the use of high frequency EPR (HF-EPR) is to accurately characterize both the spin of the ground state and the sign and magnitude of the zero-field splitting parameter D . HF-EPR spectroscopy characterization was performed on a number of polynuclear complexes. A collection of tetranuclear, heptanuclear, one-dimensional, and dodecanuclear complexes were studied. The high microwave energies employed clearly resolve the resonances arising from the transition between zero-field split energy levels of the ground state making it possible to determine both S and D values accurately.

¹ Aromi, *et al.*, Polyhedron, (1999) in press.

² Dahlberg, E.D., *et al.*, Physics Today, **34** (1995).

³ Friedman, J.R., *et al.*, J. Appl. Phys., **79**, 6031 (1996).

Collapse of the Charge-Ordered State in $\text{Nd}_{0.5}\text{Sr}_{0.5}\text{MnO}_3$: Microwave Evidences

Zvyagin, S., NHMFL

Saylor, C., NHMFL

Brunel, L.-C., NHMFL

Kamenev, K., Univ. of Edinburg, Physics and Astronomy

Lüthi, B., Univ. of Frankfurt, Institute of Physics

The recent discovery of the negative colossal magnetoresistance (CMR) in distorted perovskite manganites has attracted a considerable interest. The study of microwave properties of

CMR manganites is a relatively new topic with only a few works, which focused primarily on the resonance particularities in the manganites. The main purpose of this study was to investigate the high-frequency properties of the typical CMR-compound, $\text{Nd}_{0.5}\text{Sr}_{0.5}\text{MnO}_3$, in a broad frequency, temperature and magnetic field region of the metal-to-insulator phase transition.

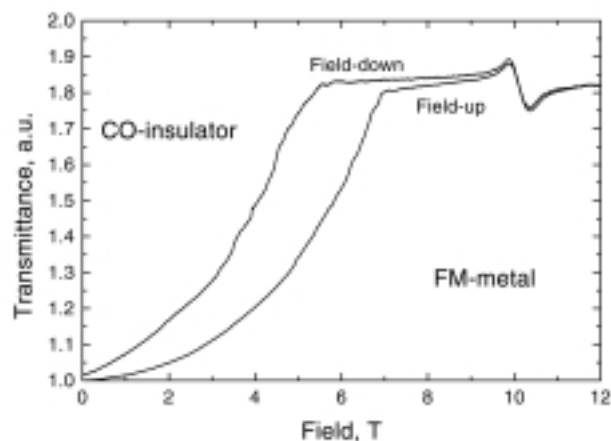


Figure 1. Signal of ESR-transmittance of $\text{Nd}_{0.5}\text{Sr}_{0.5}\text{MnO}_3$ at 288 GHz, $T = 115\text{K}$.

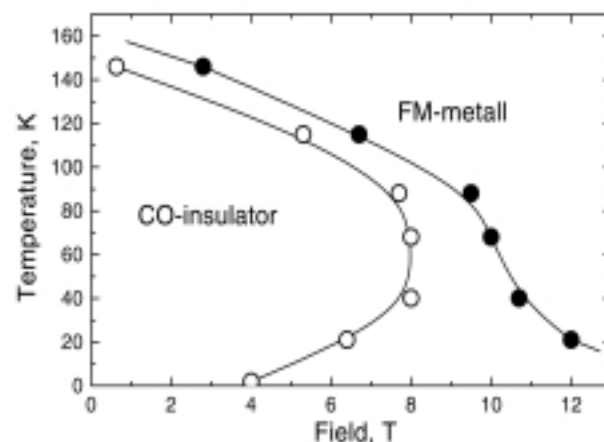


Figure 2. The temperature-field phase diagram of $\text{Nd}_{0.5}\text{Sr}_{0.5}\text{MnO}_3$ obtained from ESR (the lines are guides for eye). The closed and open circles are the fields of the insulator-to-metal and metal-to-insulator transitions accordingly.

The 50%-hole doped manganite $\text{Nd}_{0.5}\text{Sr}_{0.5}\text{MnO}_3$ was investigated using high frequency (mm-wavelength range) ESR. The temperature and field dependence of the absorption was observed below the charge ordering (CO) temperature, T_{CO}

150 K. With the transition to a metallic phase the sample demonstrated an unexpected huge (up to 80%) “blooming” (Figure 1). Magnetic field dependent hysteresis behavior of the microwave transmission anomaly conforms to previous observation of the first-order phase transition from an AFM-insulator to a FM metal;¹ the T-B diagram was obtained from the ESR experiments (Figure 2). Such an unusual behavior observed below T_{CO} clearly indicates the collapse of the CO state, induced by the external magnetic field. The resonance absorption observed in the FM phase (see Figure 1, $B = 10.4\text{ T}$) can be interpreted as a FM excitation of Mn-subsystem.

One of the possible explanation of the microwave anomaly connects with the recent observation of coexisting giant clusters of different phases in manganites.³ Such an inhomogeneous cluster structure could cause the so-called interfacial polarization (Maxwell-Wagner mechanism), which is usually characterized by a high dielectric constant and is accompanied by high loss. With the transition of the system into the metallic phase the CO state melts, the system becomes more homogeneous, allowing the microwaves to propagate with lower losses. Note that heterogeneous (composite) materials are widely used in industry as microwave insulators and as materials for quasi-optical components.⁴ From an application point a view, the unique high-frequency properties of CMR manganites may open up some possibility for microwave devices.

Acknowledgements: This work was supported in part by BMBF grant 13N 6581 and DFG through SFB 252. S. Zvyagin acknowledges support of Alexander von Humboldt Foundation.

¹ Kuwahara, H., *et al.*, Science, **270**, 961 (1995).

² Mori, S., *et al.*, Nature, **392**, 473 (1998).

³ Uehara, M., *et al.*, Nature, **399**, 560 (1999).

⁴ Von Hippel, A.R., Dielectric materials and applications, New York, 1954.

FIR Manifestation of the Metal-Insulator Phase Transition in $\text{Nd}_{0.5}\text{Sr}_{0.5}\text{MnO}_3$

Zvyagin, S., NHMFL

Wang, Y.-J., NHMFL

Brunel, L.-C., NHMFL

Kamenev, K., Univ. of Edinburg, Physics and Astronomy

The colossal magnetoresistance (CMR) in 50%-hole doped manganites is of particular interest in part because of the charge-ordering (CO) phenomena (see, for example, Ref. 1). Recent observation showing the collapse of the charge-ordered state under an applied magnetic field by means of high-frequency ESR in $\text{Nd}_{0.5}\text{Sr}_{0.5}\text{MnO}_3$ ^{2,3} has stimulated further FIR-investigations.

The FIR reflectivity of $\text{Nd}_{0.5}\text{Sr}_{0.5}\text{MnO}_3$ was studied over a broad range of magnetic fields (0 to 15 T) and wave numbers (100 to 600 cm^{-1}) at the temperature, $T = 5$ K. This experiment revealed the pronounced and unusual signature of the insulator-to-metal phase transition under an external magnetic field. A sudden decrease in the FIR reflectivity at the insulator-to-metal phase transition in $\text{Nd}_{0.5}\text{Sr}_{0.5}\text{MnO}_3$ was observed for the first time (Figure 1). Such anomalous behavior was detected in a broad frequency range and is the main result of the present research report. The FIR spectra revealed several distinct reflection features, for which the manifestations depend strongly upon the external magnetic field.

In an attempt to understand what causes the change in the FIR-spectra, we have explored two possibilities. First we considered

charge density waves (CDW) that could be excited within the stripes assuming CDW ground state in the CO phase (direct observation of the CO stripes in $(\text{La,Ca})\text{MnO}_3$ was reported recently⁴). Thus the reflection in the insulator phase shows the collective response of the CDW pinned amplitude modes.⁵ Another explanation connects to the interfacial polarization (Maxwell-Wagner mechanism), that takes place in heterogeneous dielectrics and can be characterized by extremely high dielectric constant and by high reflectivity consequently. The coexistence of the giant clusters of different phases in manganites has been observed recently in CO phase.⁶ We suggest, that such an inhomogeneous clustered structure can cause the interfacial polarization in $\text{Nd}_{0.5}\text{Sr}_{0.5}\text{MnO}_3$. With the transition of the system into FM phase the CO state melts, the system becomes more homogeneous and the FIR-reflectance drops.

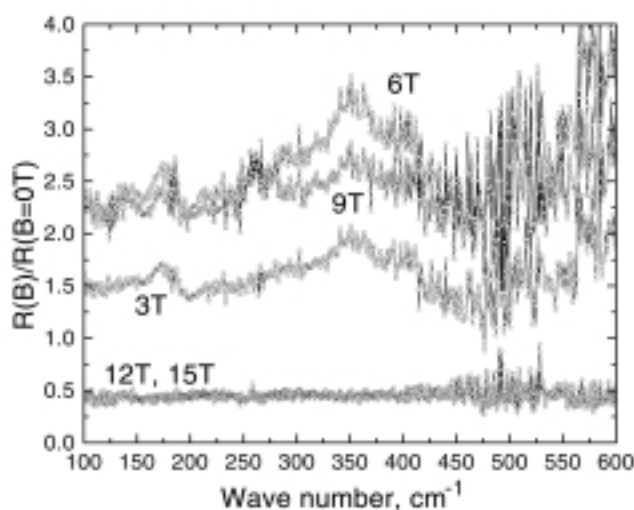


Figure 1. Reflectance ratio $R(B)/R(B=0T)$ of $\text{Nd}_{0.5}\text{Sr}_{0.5}\text{MnO}_3$ as a function of the applied field, B (the field is increasing).

We should note that the FIR-reflection spectra of $\text{Nd}_{0.5}\text{Sr}_{0.5}\text{MnO}_3$ that we observed are different from those obtained recently by Jung, *et al.*⁷ Obviously the experimental results in both cases reflect properties of the sample surface and its preparation techniques.⁸ In order to determine the bulk properties $\text{Nd}_{0.5}\text{Sr}_{0.5}\text{MnO}_3$ FIR transmission-type experiments will be extremely important. Anomalous behavior of $\text{Nd}_{0.5}\text{Sr}_{0.5}\text{MnO}_3$ in the FIR-range will be of interest for further theoretical studies.

¹ Kuwara, H., *et al.*, Science, **270**, 961 (1995).

² Zvyagin, S., *et al.*, Proc. of PPHMF-III, 216 (1998).

³ Zvyagin, S., *et al.*, NHMFL – 1999 Annual Report.

⁴ Mori, S., *et al.*, Nature, **392**, 473 (1998).

⁵ Grüner, G., Rev. of Modern Physics, **60**, 1129 (1988).

⁶ Uehara, M., *et al.*, Nature, **399**, 560 (1999).

⁷ Jung, J.H., *et al.*, to be published.

⁸ Lee, H.J., *et al.*, to be published.